Phonon-mediated Nuclear Excitation Transfer

J. Condensed Matter Nucl. Sci. 27 (2018) 97–142

Phonon-mediated Nuclear Excitation Transfer

Peter L. Hagelstein*

Massachusetts Institute of Technology, Cambridge, MA, USA

Abstract

Excitation transfer has long been of interest in biophysics, where electronic excitation is transferred from one location to another mediated by photon exchange. We are interested in the transfer of nuclear excitation mediated by phonon exchange, which according to our theoretical approach lies at the foundation of many anomalies in Condensed Matter Nuclear Science. The transfer of excitation from one site to another involves coupling to off-resonant intermediate states with either no excitation or double excitation; as such it is a quantum mechanical effect with no classical counterpart. The indirect coupling interaction can be determined from second-order perturbation theory for an electric dipole (E1) interaction, and the resulting interaction is weak due to destructive interference. We present results for resonant phonon-mediated excitation transfer based on the relativistic phonon-nuclear boost interaction identified recently. The analysis is extended to the more complicated case of magnetic dipole (M1) interactions, where fourth-order perturbation theory is needed for the interaction. We find severe destructive interference effects very much weaken the indirect interaction in both cases. Some improvement is possible due to loss; however, the improvement seems insufficient to account for the effects seen in excitation transfer experiments in our lab. To address this issue, we propose here that shifts in the off-resonant basis state energies could lead to much larger indirect interactions. The evaluation of shifts in the basis state energies is a major project, which requires the specification of the nucleon-nucleon interaction off of resonance, and the evaluation of off-resonant binding energies; these are projects to be addressed in the future. The transverse Breit interaction is given off of resonance. The resulting indirect interaction for excitation transfer is consistent with a delocalized transfer effect, and also with cooperative (Dicke) enhancements; we expect shifts in the basis state energies to lead to new models for up-conversion and down-conversion as well. Possible connections between the model and recent experimental results from excitation transfer experiments involving a ^{57}Co source on steel are discussed. We also consider incoherent excitation transfer, where the large excitation associated with the $D_2/^4$He transition is transferred to highly excited unstable states in the nuclei of the host lattice. While the mechanism was proposed many years ago to account for low-level emission of energetic alphas, there has subsequently been no clarification of mechanism associated with these experiments, which provides motivation for us to consider the possibility of confirming or rejecting the mechanism through a systematic study where the ejected particle energy is determined as a function of the nuclear mass of host lattice nuclei. The argument is extended to excitation transfer from the HD/^{3}He transition, where few MeV alpha emission may be a candidate explanation for the observations of Storms and Scanlan, and where proton emission from ^{6}Li may be a candidate explanation for the 0.79 MeV proton signal reported by Lipinski and Lipinski.
 ISSN 2227-3123

Keywords: Excitation transfer, M1 transitions, Off-resonance states, Phonon–nuclear coupling, Theory

*Corresponding author. E-mail: plh@mit.edu.

© 2018 ISCMNS. All rights reserved. ISSN 2227-3123

1. Introduction

Motivation for an interest in the problem stems from the search for an explanation for the mechanism involved in excess heat production in the Fleischmann–Pons experiment [1,2]. Since the energy produced does not come out as energetic nuclear radiation, there must be other channels involved, and from early on we have focused on the possible coupling of the nuclear energy directly into vibrations. For this to work there are a host of issues to face, including the specification of an appropriate phonon-nuclear interaction, the identification of a down-conversion mechanism through which the large nuclear quanta can be converted to the low-energy vibrational quanta, and eventually some experimental verification that the models correspond to reality [3]. Relatively recently we have identified a (somewhat obscure) relativistic interaction (the boost correction to the nuclear potential) as a candidate to provide for an appropriate phonon-nuclear interaction [4]. This mechanism allows for the exchange of vibrational quanta from the "macroscopic" lattice with nucleons of the "microscopic" internal nuclear system.

Up-conversion and down-conversion can be analyzed in simple models in which two-level systems are coupled to a common oscillator. Unfortunately, destructive interference hinders the rate at which down-conversion occurs in these models, so in order to achieve a fast down-conversion rate one needs to find a way to reduce the destructive interference. We noticed that loss processes which are antisymmetric off of resonance (different for off-resonant basis states with higher energy than for off-resonant bases states with lower energy) can remove the destructive interference, and models for up-conversion and down-conversion were quantified under conditions where the destructive interference is completely eliminated [5–9].

In these models the large energy quantum is down-converted through the sequential emission of phonons, one phonon at a time, in a great many phonon exchange processes (where each one individually involves the raising or lowering of the nuclear state) that need to be completed before coherence is lost. According to the models there are cooperative effects (Dicke enhancement) which can help if the coupling between the nuclei and a highly excited phonon mode is the same for each nucleus. Looked at two interactions at a time, this phonon exchange and nuclear raising and lowering together make up an excitation transfer step.

In recent years we have worked toward the development of new experiments that focus on providing tests of some of the theoretical statements and models in detail. Initially we worked with up-conversion experiments, but had little luck. Last year we moved to experiments focusing on excitation transfer, and observed anomalous effects [10], which have subsequently become the focus of our experimental studies. There has emerged over the last few years a new appreciation of the importance of the excitation transfer mechanism itself; as an important theoretical mechanism in its own right; as a mechanism amenable to experimental study; and with a real prospect of connecting experiment with theory. This year we have continued the experiments, but in addition have continued the theoretical studies hoping to construct models that we might compare in detail with current or with future experiments. This discussion then places excitation transfer studies into context, and provides the motivation for our focus on the problem.

In what follows our first task is to develop an introductory discussion to help bring readers from other areas up to speed with some of the basic issues associated with excitation transfer. Next we present the results of calculations of the indirect interaction associated with phonon-mediated nuclear excitation transfer first for the simplest case of electric dipole (E1) nuclear transitions, and then for the much more complicated case of magnetic dipole (M1) transitions. We have known for years that destructive interference results in a very weak indirect interaction in the E1 case, but it was not clear what the situation would be for M1 transitions. In contrast to our presentation at ICCF21, here we find that destructive interference severely impacts the indirect interaction for the M1 case as well. We have discussed many times the possibility that loss can reduce the destructive interference associated with up-conversion and down-conversion; here the approach is extended to nuclear excitation transfer, with the result that a modest improvement is obtained. This motivates us to seek other mechanisms which might reduce the destructive interference, and in this work we discuss a new mechanism that involves off-resonant shifts in the basis state energies.

Following these discussions, we turn to possible interpretations of effects seen in our excitation transfer experiments in terms of the excitation transfer models.

In the latter part of the paper we consider incoherent excitation transfer mechanisms associated with the transfer of large excitation from the $D_2/^4He$ transition and $HD/^3He$ transition to highly-excited unstable states which decay through disintegration.

Appendix A provides an enumeration of lengthy terms for one of the M1 indirect interactions. In Appendix B we provide details associated with a dynamical model for two driven nuclei in proximity coupled through resonant excitation transfer. And in Appendix C a brief discussion of internal conversion in connection with excitation transfer is given in response to a reviewer's comments.

2. Excitation Transfer

Excitation transfer of electronic excitation as a physical process was considered in the 1930s in connection with photosynthesis. A theory for photon-mediated resonant excitation transfer was given by Förster in 1948 [11], focusing on the lowest-order Coulomb dipole–dipole interaction [12]. In an idealized excitation transfer event, excitation at one site is transferred to another site. In the initial state the excitation can be thought of as being at site 1 with no excitation at site 2; and in the final state the excitation is at site 2 with no excitation remaining at site 1. We might write for an incoherent resonant excitation transfer event

$$A_1^* A_2 \;\rightarrow\; A_1 A_2^*, \tag{1}$$

where A is an excited atom or molecule. A non-resonant excitation transfer event is also possible, in which the excitation in the initial state is at a higher energy than the excitation in the final state, with the energy difference transferred to some other degree of freedom. Non-resonant excitation transfer involving phonon emission could be written as

$$A_1^* B_2 \;\rightarrow\; A_1 B_2^* + \hbar\omega_p \tag{2}$$

in which the atoms or molecules at the different sites are A and B, and where the phonon energy is $\hbar\omega_p$.

2.1. Intermediate states

In the brief discussion above we have taken advantage of a feature of the formalism specific to electromagnetism in the Coulomb gauge, where the Coulomb interaction is modeled as a simple potential, and there is no discussion of the emission or absorption of a virtual photon. However, were we to make use of a different gauge (specifically one in which the Coulomb potential is not used) then our discussion would be more complicated. In this more complicated version of the discussion, a photon would be emitted at one site coupled to a raising or lowering of the atomic or molecular state, and that same photon would be absorbed at the other site coupled to the raising or lowering of the molecular state. In this case Eq. (1) would be replaced by

$$\begin{array}{ccccc} & & A_1^* A_2^* + h\nu & & \\ & \nearrow & & \searrow & \\ A_1^* A_2 & & & & A_1 A_2^*, \\ & \searrow & & \nearrow & \\ & & A_1 A_2 + h\nu & & \end{array} \tag{3}$$

where we have used $h\nu$ for the exchanged photon. In this version of the excitation transfer process it becomes clear that the exchange is mediated by photons, and that off-resonant intermediate states are present in which both atoms or molecules are either excited or unexcited at the same time. In this resonant excitation transfer process, the system has sufficient energy to allow one atom/molecule to be excited and one unexcited (the initial and final states work this way, and they would be considered to be on resonance). One of the intermediate states has both atoms/molecules excited, and also has a photon present. The system in this case does not have sufficient energy to be in this state, so we consider it to be off-resonance. It is a virtual state. The system couples to it from both the initial state and final state, so in an excitation transfer it will have finite occupation; but its oscillatory time dependence will be that of the initial state (and/or final state) and not the time dependence it might have if the system had sufficient energy for both to be excited. We emphasize that energy is conserved from the initial state transitioning to the final state in this resonant interaction; however, energy is not conserved for the intermediate states – instead they are just off of resonance. The photon does not take up the mismatch in excitation energy.

2.2. Excitation transfer mediated by phonon exchange

It is possible for atoms and molecules in condensed matter to undergo a change of state in connection with phonon emission or absorption. In this case excitation transfer can be mediated by phonon exchange instead of photon exchange. For phonon-mediated resonant excitation transfer we might write

$$\mathrm{A}_1^*\mathrm{A}_2 + n\hbar\omega_\mathrm{p} \begin{array}{l} \nearrow \mathrm{A}_1^*\mathrm{A}_2^* + (n+1)\hbar\omega_\mathrm{p} \\ \nearrow \mathrm{A}_1^*\mathrm{A}_2^* + (n-1)\hbar\omega_\mathrm{p} \\ \searrow \mathrm{A}_1\mathrm{A}_2 + (n+1)\hbar\omega_\mathrm{p} \\ \searrow \mathrm{A}_1\mathrm{A}_2 + (n-1)\hbar\omega_\mathrm{p} \end{array} \begin{array}{l} \searrow \\ \searrow \\ \nearrow \\ \nearrow \end{array} \mathrm{A}_1\mathrm{A}_2^* + n\hbar\omega_\mathrm{p}. \tag{4}$$

Things are a little different in this case since there is the possibility that we have phonons already present in the phonon mode involved in the exchange. A phonon can be created or destroyed in connection with a raising or lowering, so now there are four intermediate states involved (at lowest order).

2.3. Toy model for phonon-mediated excitation transfer

It is possible to develop a toy model for phonon-mediated excitation transfer based on the spin–boson model for which the Hamiltonian is

$$\hat{H} = \Delta E \frac{\hat{s}_z}{\hbar} + \hbar\omega_0 \hat{a}^\dagger \hat{a} + V(\hat{a} + \hat{a}^\dagger)\frac{2\hat{s}_x}{\hbar}, \tag{5}$$

where the first term on the right-hand side accounts for the energy of the two-level system with transition energy ΔE, where the second term accounts for the simple harmonic oscillator energy, and where the third term describes a linear coupling between the two systems. In this model a phonon exchange (which can be a creation or annihilation) occurs along with a raising or lowering of the two-level system.

We are interested in a solution of the time-independent Schrödinger equation

$$E\Psi = \hat{H}\Psi \tag{6}$$

that is relevant to excitation transfer. For this we make use of a finite basis approximation in which we take a solution of the form

$$\Psi = c_1\Phi_1 + \cdot + c_6\Phi_6, \tag{7}$$

where the individual basis states are taken to be

$$\Phi_1 = |\uparrow,\downarrow,n\rangle, \quad \Phi_2 = |\downarrow,\downarrow,n-1\rangle, \quad \Phi_3 = |\downarrow,\downarrow,n+1\rangle,$$
$$\Phi_4 = |\uparrow,\uparrow,n-1\rangle, \quad \Phi_5 = |\uparrow,\uparrow,n+1\rangle, \quad \Phi_6 = |\downarrow,\uparrow,n\rangle. \tag{8}$$

The notation here works as follows: the first two-level system can be in the ground state ($\downarrow$) or in the excited state ($\uparrow$) as determined by the first entry in the ket; the second two-level system can similarly be in the ground or excited state as determined by the second entry in the ket; the third entry in the ket is the number of phonons in the oscillator.

The eigenvalue equation associated with the finite basis approximation can be written as

$$Ec_1 = n\hbar\omega_0 c_1 + V\sqrt{n}c_2 + V\sqrt{n+1}c_3 + V\sqrt{n}c_4 + V\sqrt{n+1}c_5,$$
$$Ec_2 = \Big[-\Delta E + (n-1)\hbar\omega_0\Big]c_2 + V\sqrt{n}c_1 + V\sqrt{n}c_6,$$
$$Ec_3 = \Big[-\Delta E + (n+1)\hbar\omega_0\Big]c_3 + V\sqrt{n+1}c_1 + V\sqrt{n+1}c_6,$$
$$Ec_4 = \Big[\Delta E + (n-1)\hbar\omega_0\Big]c_4 + V\sqrt{n}c_1 + V\sqrt{n}c_6,$$
$$Ec_5 = \Big[\Delta E + (n+1)\hbar\omega_0\Big]c_5 + V\sqrt{n+1}c_1 + V\sqrt{n+1}c_6,$$
$$Ec_6 = n\hbar\omega_0 c_6 + V\sqrt{n}c_2 + V\sqrt{n+1}c_3 + V\sqrt{n}c_4 + V\sqrt{n+1}c_5. \tag{9}$$

It is possible to eliminate the expansion coefficients associated with the off-resonant basis states ($c_2,\ldots,c_5$) algebraically resulting in

$$Ec_1 = n\hbar\omega_0 c_1 + \left(\frac{V^2 n}{E+\Delta E+\hbar\omega_0} + \frac{V^2(n+1)}{E+\Delta E-\hbar\omega_0} + \frac{V^2 n}{E-\Delta E+\hbar\omega_0} + \frac{V^2(n+1)}{E-\Delta E-\hbar\omega_0}\right)(c_1+c_6),$$
$$Ec_6 = n\hbar\omega_0 c_6 + \left(\frac{V^2 n}{E+\Delta E+\hbar\omega_0} + \frac{V^2(n+1)}{E+\Delta E-\hbar\omega_0} + \frac{V^2 n}{E-\Delta E+\hbar\omega_0} + \frac{V^2(n+1)}{E-\Delta E-\hbar\omega_0}\right)(c_1+c_6). \tag{10}$$

This can be recast in the form of an equivalent two-level system according to

$$Ec_1 = \Big[n\hbar\omega_0 + \Sigma_{11}(E)\Big]c_1 + V_{16}(E)c_6,$$

$$Ec_6 = \Big[n\hbar\omega_0 + \Sigma_{66}(E)\Big]c_6 + V_{61}(E)c_1, \tag{11}$$

where the self-energies are

$$\begin{aligned}\Sigma_{11}(E) = \Sigma_{66}(E) =& \frac{V^2 n}{E + \Delta E - (n-1)\hbar\omega_0} + \frac{V^2(n+1)}{E + \Delta E - (n+1)\hbar\omega_0} \\ &+ \frac{V^2 n}{E - \Delta E - (n-1)\hbar\omega_0} + \frac{V^2(n+1)}{E - \Delta E - (n+1)\hbar\omega_0}\end{aligned} \tag{12}$$

and where the indirect coupling coefficients are

$$\begin{aligned}V_{16}(E) = V_{61}(E) =& \frac{V^2 n}{E + \Delta E - (n-1)\hbar\omega_0} + \frac{V^2(n+1)}{E + \Delta E - (n+1)\hbar\omega_0} \\ &+ \frac{V^2 n}{E - \Delta E - (n-1)\hbar\omega_0} + \frac{V^2(n+1)}{E - \Delta E - (n+1)\hbar\omega_0}.\end{aligned} \tag{13}$$

We see that in this equivalent two-level system model the basis state energies depend on the eigenvalue E, as do the indirect coupling terms. If we assume that the coupling is weak, then the eigenvalue E would be close to the basis state energy of Φ_1 and Φ_6 so that

$$E \;\rightarrow\; n\hbar\omega_0. \tag{14}$$

In this case the indirect coupling matrix elements are

$$V_{16} = V_{61} \;\rightarrow\; \frac{2V^2\hbar\omega_0}{(\Delta E)^2 - (\hbar\omega_0)^2} \;\rightarrow\; \frac{2V^2\hbar\omega_0}{(\Delta E)^2}. \tag{15}$$

We see that destructive interference has led to cancellation effects so that the indirect coupling matrix element is much smaller than the individual terms contributing to it (assuming that the oscillator energy $\hbar\omega_0$ is much smaller than the transition energy ΔE), and that there is no longer any dependence on the degree of excitation of the oscillator. A version of this model is discussed briefly in Lu's thesis [13].

3. Phonon-mediated Nuclear Excitation Transfer

It was recognized that phonon-nuclear interactions can be based on a (known) boost correction for the strong force inside of a moving (and accelerating or oscillating) nucleus [4]. We are motivated in this section to exercise this theory by applying it to excitation transfer. For simplicity in this section we focus on nuclear E1 transitions for which only a single phonon exchange is coupled to a nuclear transition. Some discussion of this problem was given previously in Ref. [14].

3.1. Nuclear and phonon Hamiltonian

To describe the internal nuclear states, the phonon modes, and the phonon-nuclear coupling in general we can make use of the Hamiltonian [15,16]

$$\hat{H} = \sum_j \mathbf{M}_j c^2 + \sum_j \mathbf{a}_j \cdot c\hat{\mathbf{P}}_j + \sum_{\mathbf{k},\sigma} \hbar\omega_{\mathbf{k},\sigma} \hat{a}^\dagger_{\mathbf{k},\sigma} \hat{a}_{\mathbf{k},\sigma}. \tag{16}$$

The first term on the RHS describes the internal nuclear energy in a finite basis approximation, where the mass matrix $\mathbf{M}_j$ for the nucleus at lattice site j is a diagonal matrix with the individual nuclear state masses as entries. The mass energy of a particular nuclear state $|J,m\rangle$ is

$$(E_{Jm})_j = (M_{Jm,Jm}c^2)_j. \tag{17}$$

The last term on the right-hand side describes the vibrational energy in a mode expansion, where $\hbar\omega_{\mathbf{k},\sigma}$ is the energy of a phonon with momentum $\hbar\mathbf{k}$ with polarization denoted by σ. The middle term on the right-hand side accounts for the relativistic phonon-nuclear interaction, where the $\mathbf{a}$ matrix contains off-diagonal entries given by [4]

$$\left(\mathbf{a}_{Jm,J'm'} \cdot c\hat{\mathbf{P}}\right)_j = \left\langle J,m \left| \frac{1}{M} \sum_k \beta_k \hat{\mathbf{P}}_j \cdot \hat{\boldsymbol{\pi}}_k + \frac{1}{2Mc} \sum_{k<l} \left[(\beta_k \boldsymbol{\alpha}_k + \beta_l \boldsymbol{\alpha}_l) \cdot \hat{\mathbf{P}}_j, \hat{V}_{kl} \right] \right| J',m' \right\rangle \tag{18}$$

for a two-particle nuclear potential model, following the derivation and notation of Ref. [4]. M in this formula is the nuclear mass, where the difference in mass between the two states is presumed small relative to the total mass. The momentum operator $\hat{\mathbf{P}}_j$ for a monatomic lattice is

$$\hat{\mathbf{P}}_j = \sum_{\mathbf{k},\sigma} \mathbf{u}_{\mathbf{k},\sigma} \sqrt{\frac{M\hbar\omega_{\mathbf{k},\sigma}}{2N}} \left(\frac{\hat{a}_{\mathbf{k},\sigma} \mathbf{e}^{i\mathbf{k}\cdot\mathbf{R}^{(0)}_j} - \hat{a}^\dagger_{\mathbf{k},\sigma} \mathbf{e}^{-i\mathbf{k}\cdot\mathbf{R}^{(0)}_j}}{i} \right). \tag{19}$$

The equilibrium position of the center of mass for a nucleus at site j is $\mathbf{R}^{(0)}_j$.

3.2. Reduced Hamiltonian

Since the phonon-nuclear interaction has E1 symmetry for the nuclear transition, only a single nuclear transition is needed at each of the two sites in order to complete an excitation transfer. Consequently we only need to keep track of these two nuclear states, which allows for a significant reduction of the Hamiltonian. Unfortunately we cannot make use of the standard two-level system machinery, since each of the nuclear states will have a number of degenerate levels which need to be accounted for. The resulting reduced Hamiltonian can be written as

$$\begin{aligned}\hat{H} = &\sum_k \hbar\omega_k \hat{a}^\dagger_k \hat{a}_k + \sum_j \sum_{m_0} (|J_0 m_0\rangle M_0 c^2 \langle J_0 m_0|)_j + \sum_j \sum_{m_1} (|J_1 m_1\rangle M_1 c^2 \langle J_1 m_1|)_j \\ &+ \sum_j \sum_{m_0} \sum_{m_1} \left(|J_0 m_0\rangle\langle J_0 m_0|\mathbf{a}_j|J_1 m_1\rangle\langle J_1 m_1| + |J_1 m_1\rangle\langle J_1 m_1|\mathbf{a}_j|J_0 m_0\rangle\langle J_0 m_0| \right) \\ &\cdot c \sum_{\mathbf{k},\sigma} \mathbf{u}_{\mathbf{k},\sigma} \sqrt{\frac{\hbar M\omega_{\mathbf{k},\sigma}}{2N}} \left(\frac{\hat{a}_{\mathbf{k},\sigma} \mathbf{e}^{i\mathbf{k}\cdot\mathbf{R}^{(0)}_j} - \hat{a}^\dagger_{\mathbf{k},\sigma} \mathbf{e}^{-i\mathbf{k}\cdot\mathbf{R}^{(0)}_j}}{i} \right),\end{aligned} \tag{20}$$

where we focus on the ground state $|J_0, m_0\rangle$ and an excited state $|J_1, m_1\rangle$.

3.3. Phonon-nuclear interaction as a perturbation

The reduced Hamiltonian in the previous section can be recast as

$$\hat{H} = \hat{H}_0 + \hat{V}, \tag{21}$$

where $\hat{H}_0$ describes the unperturbed system

$$\hat{H}_0 = \sum_k \hbar\omega_k \hat{a}_k^\dagger \hat{a}_k + \sum_j \sum_{m_0} (|J_0 m_0\rangle M_0 c^2 \langle J_0 m_0|)_j + \sum_j \sum_{m_1} (|J_1 m_1\rangle M_1 c^2 \langle J_1 m_1|)_j \tag{22}$$

and where $\hat{V}$ describes the perturbation

$$\begin{aligned}\hat{V} = &\sum_j \sum_{m_0} \sum_{m_1} \left(|J_0 m_0\rangle\langle J_0 m_0|\mathbf{a}_j|J_1 m_1\rangle\langle J_1 m_1| + |J_1 m_1\rangle\langle J_1 m_1|\mathbf{a}_j|J_0 m_0\rangle\langle J_0 m_0| \right) \\ &\cdot c \sum_{\mathbf{k},\sigma} \mathbf{u}_{\mathbf{k},\sigma} \sqrt{\frac{\hbar M \omega_{\mathbf{k},\sigma}}{2N}} \left(\frac{\hat{a}_{\mathbf{k},\sigma} \mathbf{e}^{i\mathbf{k}\cdot\mathbf{R}_j^{(0)}} - \hat{a}_{\mathbf{k},\sigma}^\dagger \mathbf{e}^{-i\mathbf{k}\cdot\mathbf{R}_j^{(0)}}}{i} \right).\end{aligned} \tag{23}$$

3.4. Formal second-order interaction

A nice feature of this formalism is that we are able to develop operators that describe the second-order as well as higher-order interactions within the perturbation theory explicitly. At second-order we can write

$$\hat{V}_2 = \hat{V}(E - \hat{H}_0)^{-1}\hat{V}. \tag{24}$$

Excitation transfer at second-order is described by this operator (along with other effects). We can think of the $\hat{V}$ at the right of the right-hand side when it operates on an initial state as either raising or lower the nuclear state at a site while creating or destroying a phonon. The intermediate state that results is off of resonance, and the off-resonant denominator keeps track of how far and in which direction off of resonance intermediate states are. The $\hat{V}$ operator on the left of the right-hand side then raises or lowers the nuclear state at possibly a different site, also while creating or destroying a phonon.

3.5. Resonant second-order interaction

After a significant computation and taking into account that the Brillouin zone is symmetric it is possible to isolate the resonant part of the second-order interaction relevant to excitation transfer; we can write

$$\left(\hat{V}(E - \hat{H}_0)^{-1}\hat{V}\right)_{\text{resonant}} \rightarrow \frac{Mc^2}{(\Delta E)^2} \sum_{j<j'} \sum_{m_0} \sum_{m_1} \sum_{m_0'} \sum_{m_1'} \left(|J_0 m_0\rangle\langle J_1 m_1| \right)_j \left(|J_1 m_1'\rangle\langle J_0 m_0'| \right)_{j'}$$

$$\langle J_0 m_0|\mathbf{a}_j|J_1 m_1\rangle \cdot \left[\frac{1}{N}\sum_{\mathbf{k},\sigma}(\hbar\omega_{\mathbf{k},\sigma})^2 \mathbf{u}_{\mathbf{k},\sigma}\mathbf{u}_{\mathbf{k},\sigma}\cos\left(\mathbf{k}\cdot(\mathbf{R}_{j'}^{(0)}-\mathbf{R}_j^{(0)})\right)\right]\cdot\langle J_1 m_1'|\mathbf{a}_{j'}|J_0 m_0'\rangle$$

$$+\frac{Mc^2}{(\Delta E)^2}\sum_{j<j'}\sum_{m_0}\sum_{m_1}\sum_{m_0'}\sum_{m_1'}\Big(|J_1 m_1\rangle\langle J_0 m_0|\Big)_j\Big(|J_0 m_0'\rangle\langle J_1 m_1'|\Big)_{j'}$$

$$\langle J_1 m_1|\mathbf{a}_j|J_0 m_0\rangle \cdot \left[\frac{1}{N}\sum_{\mathbf{k},\sigma}(\hbar\omega_{\mathbf{k},\sigma})^2 \mathbf{u}_{\mathbf{k},\sigma}\mathbf{u}_{\mathbf{k},\sigma}\cos\left(\mathbf{k}\cdot(\mathbf{R}_{j'}^{(0)}-\mathbf{R}_j^{(0)})\right)\right]\cdot\langle J_0 m_0'|\mathbf{a}_{j'}|J_1 m_1'\rangle\Big\}. \quad (25)$$

We see in this expression a similar degree of cancellation as we found in the toy model considered above. Destructive interference has led to the cancellation of all lowest-order terms, and there does not remain any dependence on the number of phonons in the different phonon modes. Contributions from high-frequency phonon modes dominates this interaction.

3.6. Discussion

There exist many stable isotopes with E1 transitions from the ground state, for which this kind of model might apply. A list of the low energy transitions is presented in Table 1. For both the toy model and for the resonant second-order interaction above one finds the transition energy in the denominator, which would suggest our focus should be on nuclei with the lowest energy transitions from the ground state. In this case the 6.237 keV transition in ^{181}Ta is favored.

We have evaluated the contribution to the $\hat{\mathbf{a}}$-matrix element for the 6.237 keV transition of ^{181}Ta from the boosted spin-orbit interaction, making use of a single proton model in a deformed potential model. The result we obtained that the magnitude is on the order of 10^{-6} – a result which indicates that this contribution is weak.

One approach to testing for this kind of excitation transfer effect might be to look for angular anisotropy in the gamma emission from excited state ^{181}Ta(6237 keV) in crystalline Ta. A computation of the summation over the different phonon modes indicates that we would expect a weak excitation transfer dominated by transfer to the nearest neighbors. Making use of the indirect coupling formula given above and our estimate for the indirect matrix element, we might expect it possible to see a deviation from the isotropic case on the order of 10^{-3}. Given the relative weakness of emission of the 6.237 keV gamma, such an experiment would be expected to be technically challenging.

Table 1. Low-energy electric dipole (E1) transitions from the ground state of stable nuclei, from the BNL Nudat2 database. The internal conversion coefficient is α.

Isotope	E(keV)	$T_{1/2}$	Multipolarity	α
Ta-181	6.237	6.05 μsec	E1	70.5
Dy-161	25.65135	29.1 ns	E1	2.29
Gd-157	63.929	0.46 μsec	E1	0.961
Dy-161	74.56668	3.14 ns	E1	0.672
Gd-155	86.5479	6.50 ns	E1	0.434
Eu-153	97.43100	0.198 ns	E1	0.307
Dy-161	103.062	0.60 ns	E1	0.285
Gd-155	105.3083	1.16 ns	E1	0.256
F-19	109.9	0.591 ns	E1	
Dy-161	131.8	0.145 ns	[E1]	0.1475
Eu-153	151.6245	0.36 ns	E1	0.092

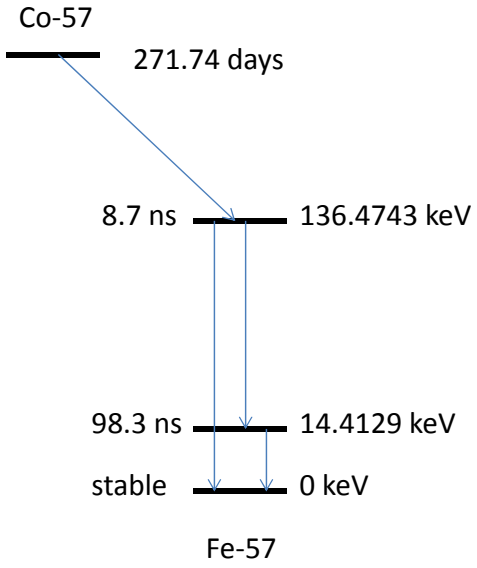

Figure 1. Simplified version of the nuclear decay scheme for Co-57; energy levels and half-life times are from the Nudat2 online data base of Brookhaven National Lab.

4. Excitation Transfer for M1 and E2 Transitions

The development of an excitation transfer experiment in ^{181}Ta based on the production of excited state nuclei from the decay of a radioactive source is problematic due to difficulties acquiring radioactive ^{181}W. Consequently in our lab we have focused on experiments involving excited states of ^{57}Fe that are populated from the decay of the more readily available radioactive ^{57}Co [10,13]. The primary decay path following electron capture associated with the beta decay of the ^{57}Co nucleus is shown in Fig. 1. Transitions from the ground state to the 14.4 keV state and 136.5 keV state are M1+E2, with the magnetic dipole (M1) contribution dominant, and the electric quadrupole (E2) contribution much weaker.

Since the phonon–nuclear interaction of the boost correction involves an E1 nuclear transition, in order to couple between the ground state and lowest excited states in ^{57}Fe we will need two phonon exchanges and intermediate states that couple through individual single phonon E1 transitions. A model for excitation transfer in this case will be more complicated since the lowest-order contribution will involve the exchange of four phonons.

This provides a new problem on which we might exercise the new phonon-nuclear theory. We are encouraged in that we appear to be seeing changes in X-ray and gamma emission consistent with the presence of excitation transfer in experiments. However, it is discouraging that the lowest-order interaction in the E1 version of the problem leads to such a weak indirect interaction.

At ICCF21 we described some preliminary results suggesting that destructive interference was not as bad in the M1 problem than in the E1 problem described in the previous section. The issue here is that since the models and calculations are new, with essentially no relevant previous work done on them, it is not obvious at the outset whether excitation in the M1 transition will be qualitatively different. A detailed and debugged version of the calculation is needed to provide clarification. Months after the conference a new set of calculations have been carried out, with the result that destructive interference indeed results in very weak indirect interactions. In this section we will provide a

brief review of the issues and associated calculations. The conclusion to be drawn is that the most straightforward and simplest application of the theory does not lead to predictions consistent with experiment. This will motivate us to consider modifications of the model in subsequent sections.

4.1. Simple classification of the interactions

Excitation transfer in the E1 case is particularly simple in that there is only a single transition and a single phonon mode involved for any specific contributing term at second order in perturbation theory. However, for the M1 and E2 cases, two different transitions are involved for each nucleus, and phonon exchange can occur with one phonon mode, two phonon modes, or three different phonon modes. We have carried out calculations systematically for all cases, and find that each case has its own technical issues and peculiarities in the computations, and leads to different expected behavior at the end. In what follows we summarize the essential results for the different cases.

4.2. Reduced version of the Hamiltonian

We make use of the same phonon–nuclear Hamiltonian as before in Equation (16), but this time we make use of an expanded subset given by

$$\begin{aligned}
\hat{H} =& \sum_k \hbar\omega_k \hat{a}_k^\dagger \hat{a}_k + \sum_j \sum_{m_0} (|J_0 m_0\rangle M_0 c^2 \langle J_0 m_0|)_j \\
&+ \sum_j \sum_{m_1} (|J_1 m_1\rangle M_1 c^2 \langle J_1 m_1|)_j + \sum_j \sum_{J_2} \sum_{m_2} (|J_2 m_2\rangle M_2 c^2 \langle J_2 m_2|)_j \\
&+ \sum_j \sum_{m_0} \sum_{J_2} \sum_{m_2} \left(|J_0 m_0\rangle\langle J_0 m_0|\mathbf{a}_j|J_2 m_2\rangle\langle J_2 m_2| + |J_2 m_2\rangle\langle J_2 m_2|\mathbf{a}_j|J_0 m_0\rangle\langle J_0 m_0| \right) \\
&\quad \cdot c \sum_{\mathbf{k},\sigma} \mathbf{u}_{\mathbf{k},\sigma} \sqrt{\frac{\hbar M \omega_{\mathbf{k},\sigma}}{2N}} \left(\frac{\hat{a}_{\mathbf{k},\sigma} \mathbf{e}^{i\mathbf{k}\cdot\mathbf{R}_j^{(0)}} - \hat{a}_{\mathbf{k},\sigma}^\dagger \mathbf{e}^{-i\mathbf{k}\cdot\mathbf{R}_j^{(0)}}}{i} \right) \\
&+ \sum_j \sum_{m_1} \sum_{J_2} \sum_{m_2} \left(|J_1 m_1\rangle\langle J_1 m_1|\mathbf{a}_j|J_2 m_2\rangle\langle J_2 m_2| + |J_2 m_2\rangle\langle J_2 m_2|\mathbf{a}_j|J_1 m_1\rangle\langle J_1 m_1| \right) \\
&\quad \cdot c \sum_{\mathbf{k},\sigma} \mathbf{u}_{\mathbf{k},\sigma} \sqrt{\frac{\hbar M \omega_{\mathbf{k},\sigma}}{2N}} \left(\frac{\hat{a}_{\mathbf{k},\sigma} \mathbf{e}^{i\mathbf{k}\cdot\mathbf{R}_j^{(0)}} - \hat{a}_{\mathbf{k},\sigma}^\dagger \mathbf{e}^{-i\mathbf{k}\cdot\mathbf{R}_j^{(0)}}}{i} \right) .
\end{aligned} \tag{26}$$

The nuclear ground state is denoted by $|J_0, m_0\rangle$, the (relatively low-energy) nuclear excited state is denoted by $|J_1, m_1\rangle$, and (much higher energy) nuclear intermediate states are denoted by $|J_2, m_2\rangle$. Included in this restricted Hamiltonian are transitions between the ground state, and the low-energy excited state, to high-energy intermediate states; but no transitions directly between the ground state and low-energy excited state.

4.3. Interaction in the case of one phonon mode

In this case we make use of fourth-order perturbation theory and assume that the phonon energy is small compared to the nuclear transition energy. A great many terms are involved, and we made use of the symbolic algebra program

Mathematica for all of the algebra. We wrote a computer code that put together an input file for Mathematica which enumerated all states, couplings, and contributing pathways.

The resonant part of the fourth-order interaction involving a single phonon mode which has a non-trivial spatial dependence can be written as

$$\left(\hat{V}(E-\hat{H}_0)^{-1}\hat{V}(E-\hat{H}_0)^{-1}\hat{V}(E-\hat{H}_0)^{-1}\hat{V}\right)_{\rm resonant} \rightarrow$$
$$\frac{(Mc^2)^2}{4N}\sum_{J_2}\sum_{J_2'}\frac{\left(\begin{array}{c}(E_1-E_0)^2-3(E_1-E_0)[(E_2-E_0)+(E_2'-E_0)]\\ +2[(E_2-E_0)^2+(E_2-E_0)(E_2'-E_0)+(E_2'-E_0)^2]\end{array}\right)}{(E_2-E_0)(E_2'-E_0)(E_1-E_2)(E_1-E_2')(E_2+E_2'-E_0-E_1)}$$
$$\sum_j\sum_{j'}\sum_{m_0}\sum_{m_1}\sum_{m_2}\sum_{m_0'}\sum_{m_1'}\sum_{m_2'}\left(|J_0m_0\rangle\langle J_1m_1|\right)_j\left(|J_1m_1'\rangle\langle J_0m_0'|\right)_{j'}$$
$$\sum_\alpha\sum_\beta\sum_\gamma\sum_\delta(\langle J_0m_0|\mathbf{a}_j|J_2m_2\rangle)_\alpha(\langle J_2m_2|\mathbf{a}_j|J_1m_1\rangle)_\beta(\langle J_1m_1'|\mathbf{a}_{j'}|J_2'm_2'\rangle)_\gamma(\langle J_2'm_2'|\mathbf{a}_{j'}|J_0m_0'\rangle)_\delta$$
$$\left[\frac{1}{N}\sum_{\mathbf{k},\sigma}(\hbar\omega_{\mathbf{k},\sigma})^2(\mathbf{u}_{\mathbf{k},\sigma})_\alpha(\mathbf{u}_{\mathbf{k},\sigma})_\beta(\mathbf{u}_{\mathbf{k},\sigma})_\gamma(\mathbf{u}_{\mathbf{k},\sigma})_\delta\cos\left(2\mathbf{k}(\mathbf{R}_{j'}^{(0)}-\mathbf{R}_j^{(0)})\right)\right]$$
$$+i\frac{(Mc^2)^2}{2N}\sum_{J_2}\sum_{J_2'}\frac{(2E_2-E_0-E_1)(2E_2'-E_0-E_1)}{(E_1-E_0)(E_2-E_0)(E_2'-E_0)(E_2-E_1)(E_2'-E_1)}$$
$$\sum_j\sum_{j'}\sum_{m_0}\sum_{m_1}\sum_{m_2}\sum_{m_0'}\sum_{m_1'}\sum_{m_2'}\left(|J_0m_0\rangle\langle J_1m_1|\right)_j\left(|J_1m_1'\rangle\langle J_0m_0'|\right)_{j'}$$
$$\sum_\alpha\sum_\beta\sum_\gamma\sum_\delta(\langle J_0m_0|\mathbf{a}_j|J_2m_2\rangle)_\alpha(\langle J_2m_2|\mathbf{a}_j|J_1m_1\rangle)_\beta(\langle J_1m_1'|\mathbf{a}_{j'}|J_2'm_2'\rangle)_\gamma(\langle J_2'm_2'|\mathbf{a}_{j'}|J_0m_0'\rangle)_\delta$$
$$\left[\frac{1}{N}\sum_{\mathbf{k},\sigma}(\hbar\omega_{\mathbf{k},\sigma})^2(\mathbf{u}_{\mathbf{k},\sigma})_\alpha(\mathbf{u}_{\mathbf{k},\sigma})_\beta(\mathbf{u}_{\mathbf{k},\sigma})_\gamma(\mathbf{u}_{\mathbf{k},\sigma})_\delta\hat{n}_{\mathbf{k},\sigma}\sin\left(2\mathbf{k}(\mathbf{R}_{j'}^{(0)}-\mathbf{R}_j^{(0)})\right)\right]. \quad (27)$$

We see two basic terms. The first describes a weak interaction that is independent of the number of phonons is a mode, and which is localized to nearest neighbors. The second term describes a weak interaction that is linear in the number of phonons in a mode, and which contributes as long as the phonon occupation is asymmetric with the wave vector $\mathbf{k}$. Since the phonon distribution appears in the summation over the phonon modes, it is possible in this case for excitation transfer to involve nuclei considerably more distant than nearest neighbors. We note that a quantitative evaluation of this formula will require in principle summations over all intermediate E1-coupled states.

These terms are much smaller than those appearing in the case of second-order E1 excitation transfer, due in part to the destructive interference, and in part to the effect occurring at higher-order in perturbation theory.

4.4. Interaction in the case of two phonon modes

In the case of excitation transfer where phonon exchange with two different phonon modes occurs, we require that each mode exchange a phonon with both nuclei. In this case the resonant contribution at fourth order is calculated to be

$$\left(\hat{V}(E-\hat{H}_0)^{-1}\hat{V}(E-\hat{H}_0)^{-1}\hat{V}(E-\hat{H}_0)^{-1}\hat{V}\right)_{\rm resonant} \rightarrow T_1+T_2+T_3+T_4, \quad (28)$$

where

$$T_1 = \frac{(Mc^2)^2}{4} \sum_{J_2} \sum_{J_2'} \frac{2}{(E_1 - E_0)^2 (E_2 - E_0)(E_2' - E_1)}$$

$$\sum_j \sum_{j'} \sum_{m_0} \sum_{m_1} \sum_{m_2} \sum_{m_0'} \sum_{m_1'} \sum_{m_2'} \left(|J_0 m_0\rangle\langle J_1 m_1| \right)_j \left(|J_1 m_1'\rangle\langle J_0 m_0'| \right)_{j'}$$

$$\langle J_0 m_0 | \mathbf{a}_j | J_2 m_2 \rangle \cdot \left[\frac{1}{N} \sum_{\mathbf{k},\sigma} \hbar\omega_{\mathbf{k},\sigma} \mathbf{u}_{\mathbf{k},\sigma} \mathbf{u}_{\mathbf{k},\sigma} (2\hat{n}_{\mathbf{k},\sigma} + 1) \cos\left(\mathbf{k} \cdot (\mathbf{R}_{j'}^{(0)} - \mathbf{R}_j^{(0)}) \right) \right] \cdot \langle J_1 m_1' | \mathbf{a}_{j'} | J_2' m_2' \rangle$$

$$\langle J_2 m_2 | \mathbf{a}_j | J_1 m_1 \rangle \cdot \left[\frac{1}{N} \sum_{\mathbf{k}',\sigma'} (\hbar\omega_{\mathbf{k}',\sigma'})^2 \mathbf{u}_{\mathbf{k}',\sigma'} \mathbf{u}_{\mathbf{k}',\sigma'} \cos\left(\mathbf{k}' \cdot (\mathbf{R}_{j'}^{(0)} - \mathbf{R}_j^{(0)}) \right) \right] \cdot \langle J_2' m_2' | \mathbf{a}_{j'} | J_0 m_0' \rangle \tag{29}$$

$$T_2 = \frac{(Mc^2)^2}{4} \sum_{J_2} \sum_{J_2'} \frac{2}{(E_1 - E_0)^2 (E_2' - E_0)(E_2 - E_1)}$$

$$\sum_j \sum_{j'} \sum_{m_0} \sum_{m_1} \sum_{m_2} \sum_{m_0'} \sum_{m_1'} \sum_{m_2'} \left(|J_0 m_0\rangle\langle J_1 m_1| \right)_j \left(|J_1 m_1'\rangle\langle J_0 m_0'| \right)_{j'}$$

$$\langle J_0 m_0 | \mathbf{a}_j | J_2 m_2 \rangle \cdot \left[\frac{1}{N} \sum_{\mathbf{k},\sigma} (\hbar\omega_{\mathbf{k},\sigma})^2 \mathbf{u}_{\mathbf{k},\sigma} \mathbf{u}_{\mathbf{k},\sigma} \cos\left(\mathbf{k} \cdot (\mathbf{R}_{j'}^{(0)} - \mathbf{R}_j^{(0)}) \right) \right] \cdot \langle J_1 m_1' | \mathbf{a}_{j'} | J_2' m_2' \rangle$$

$$\langle J_2 m_2 | \mathbf{a}_j | J_1 m_1 \rangle \cdot \left[\frac{1}{N} \sum_{\mathbf{k}',\sigma'} \hbar\omega_{\mathbf{k}',\sigma'} \mathbf{u}_{\mathbf{k}',\sigma'} \mathbf{u}_{\mathbf{k}',\sigma'} (2\hat{n}_{\mathbf{k}',\sigma'} + 1) \cos\left(\mathbf{k}' \cdot (\mathbf{R}_{j'}^{(0)} - \mathbf{R}_j^{(0)}) \right) \right] \cdot \langle J_2' m_2' | \mathbf{a}_{j'} | J_0 m_0' \rangle \tag{30}$$

$$T_3 = \frac{(Mc^2)^2}{4} \sum_{J_2} \sum_{J_2'} \frac{2}{(E_1 - E_0)^2 (E_2 - E_0)(E_2' - E_0)}$$

$$\sum_j \sum_{j'} \sum_{m_0} \sum_{m_1} \sum_{m_2} \sum_{m_0'} \sum_{m_1'} \sum_{m_2'} \left(|J_0 m_0\rangle\langle J_1 m_1| \right)_j \left(|J_1 m_1'\rangle\langle J_0 m_0'| \right)_{j'}$$

$$\langle J_0 m_0 | \mathbf{a}_j | J_2 m_2 \rangle \cdot \left[\frac{1}{N} \sum_{\mathbf{k},\sigma} \hbar\omega_{\mathbf{k},\sigma} \mathbf{u}_{\mathbf{k},\sigma} \mathbf{u}_{\mathbf{k},\sigma} (2\hat{n}_{\mathbf{k},\sigma} + 1) \cos\left(\mathbf{k} \cdot (\mathbf{R}_{j'}^{(0)} - \mathbf{R}_j^{(0)}) \right) \right] \cdot \langle J_2' m_2' | \mathbf{a}_{j'} | J_0 m_0' \rangle$$

$$\langle J_2 m_2 | \mathbf{a}_j | J_1 m_1 \rangle \cdot \left[\frac{1}{N} \sum_{\mathbf{k}',\sigma'} (\hbar\omega_{\mathbf{k}',\sigma'})^2 \mathbf{u}_{\mathbf{k}',\sigma'} \mathbf{u}_{\mathbf{k}',\sigma'} \cos\left(\mathbf{k}' \cdot (\mathbf{R}_{j'}^{(0)} - \mathbf{R}_j^{(0)}) \right) \right] \cdot \langle J_1 m_1' | \mathbf{a}_{j'} | J_2' m_2' \rangle \tag{31}$$

$$T_4 = \frac{(Mc^2)^2}{4} \sum_{J_2} \sum_{J_2'} \frac{2}{(E_1 - E_0)^2 (E_2 - E_1)(E_2' - E_1)}$$

$$\sum_j \sum_{j'} \sum_{m_0} \sum_{m_1} \sum_{m_2} \sum_{m_0'} \sum_{m_1'} \sum_{m_2'} \left(|J_0 m_0\rangle\langle J_1 m_1| \right)_j \left(|J_1 m_1'\rangle\langle J_0 m_0'| \right)_{j'}$$

$$\langle J_0 m_0 | \mathbf{a}_j | J_2 m_2 \rangle \cdot \left[\frac{1}{N} \sum_{\mathbf{k},\sigma} (\hbar\omega_{\mathbf{k},\sigma})^2 \mathbf{u}_{\mathbf{k},\sigma} \mathbf{u}_{\mathbf{k},\sigma} \cos\left(\mathbf{k} \cdot (\mathbf{R}_{j'}^{(0)} - \mathbf{R}_j^{(0)}) \right) \right] \cdot \langle J_2' m_2' | \mathbf{a}_{j'} | J_0 m_0' \rangle$$

$$\langle J_2 m_2 | \mathbf{a}_j | J_1 m_1 \rangle \cdot \left[\frac{1}{N} \sum_{\mathbf{k}',\sigma'} \hbar\omega_{\mathbf{k}',\sigma'} \mathbf{u}_{\mathbf{k}',\sigma'} \mathbf{u}_{\mathbf{k}',\sigma'} (2\hat{n}_{\mathbf{k}',\sigma'} + 1) \cos\left(\mathbf{k}' \cdot (\mathbf{R}_{j'}^{(0)} - \mathbf{R}_j^{(0)}) \right) \right] \cdot \langle J_1 m_1' | \mathbf{a}_{j'} | J_2' m_2' \rangle. \tag{32}$$

In this case destructive interference has resulted in a very weak interaction which depends on the symmetric part of the phonon distribution in the different modes. The indirect interaction that results is dominated by coupling to nearest neighbors. Once again it is the high-frequency phonon modes which provide the strongest contributions to the interaction.

4.5. Interaction in the case of three phonon modes

For an excitation transfer process involving three phonon modes, we require one mode to be involved in phonon exchange at both sites, and a single phonon exchange with the other modes, one at one site, and one at the other. We are most interested in resonant excitation transfer, which in the case of three modes is potentially problematic since constraints are imposed on the mode energies. For the specific interaction under consideration here, we focus on interactions in which single phonon creation and annihilation occurs for the first mode; for the second mode we require that the phonon interaction involves the creation of a phonon; and for the third mode we require phonon annihilation. Overall the interaction is resonant if the phonon mode energy is matched for the second and third mode. While not exhaustive, this provides a check to see whether or not destructive interference causes a substantial reduction of the strength of the indirect interaction in one case.

The associated contribution to the resonant indirect interaction can be written as

$$\left(\hat{V}(E-\hat{H}_0)^{-1}\hat{V}(E-\hat{H}_0)^{-1}\hat{V}(E-\hat{H}_0)^{-1}\hat{V}\right)_{\rm resonant} \rightarrow T_1' + \cdots + T_8', \tag{33}$$

where we exhibit the first contribution T_1' explicitly here

$$\begin{aligned}
T_1' = \frac{(Mc^2)^2}{4}\sum_{J_2}\sum_{J_2'}\frac{2}{(E_1-E_0)^2(E_2-E_1)(E_2'-E_1)} \\
\sum_j\sum_{j'}\sum_{m_0}\sum_{m_1}\sum_{m_2}\sum_{m_0'}\sum_{m_1'}\sum_{m_2'}\left(|J_0m_0\rangle\langle J_1m_1|\right)_j\left(|J_1m_1'\rangle\langle J_0m_0'|\right)_{j'} \\
\langle J_0m_0|\mathbf{a}_j|J_2m_2\rangle\cdot\left[\frac{1}{N}\sum_{\mathbf{k},\sigma}(\hbar\omega_{\mathbf{k},\sigma})^2\mathbf{u}_{\mathbf{k},\sigma}\mathbf{u}_{\mathbf{k},\sigma}\cos\left(\mathbf{k}\cdot(\mathbf{R}_{j'}^{(0)}-\mathbf{R}_j^{(0)})\right)\right]\cdot\langle J_2'm_2'|\mathbf{a}_{j'}|J_0m_0'\rangle \\
\langle J_2m_2|\mathbf{a}_j|J_1m_1\rangle\cdot\left[\sum_{\mathbf{k}',\sigma'}\sqrt{\hbar\omega_{\mathbf{k}',\sigma'}}\mathbf{u}_{\mathbf{k}',\sigma'}\sqrt{\hat{n}_{\mathbf{k}',\sigma'}+1}\mathrm{e}^{-i\mathbf{k}'\cdot\mathbf{R}_j^{(0)}}\right] \\
\langle J_1m_1'|\mathbf{a}_{j'}|J_2'm_2'\rangle\cdot\left[\sum_{\mathbf{k}'',\sigma''}\sqrt{\hbar\omega_{\mathbf{k}'',\sigma''}}\mathbf{u}_{\mathbf{k}'',\sigma''}\sqrt{\hat{n}_{\mathbf{k}'',\sigma''}}\mathrm{e}^{i\mathbf{k}''\cdot\mathbf{R}_{j'}^{(0)}}\right]
\end{aligned} \tag{34}$$

with the remaining terms listed in Appendix A. The resulting interaction is very weak, and localized to nearest neighbors.

4.6. Discussion

The low energy M1 transitions are of interest to us since we appear to be seeing anomalies associated with excitation transfer in experiments. A list of nuclei with low energy M1 and M1+E2 transitions is presented in Table 2. In connection with this list we draw attention to the special case of the low-energy M1+E2 transition in ^{201}Hg at 1.565 keV,

Table 2. Low-energy M1 and M1+E2 transitions from the ground state of stable nuclei, from the BNL Nudat2 database. The internal conversion coefficient is α.

Isotope	E(keV)	$T_{1/2}$	Multipolarity	α
Hg-201	1.5648	81 ns	M1+E2	4.7×10^4
Tm-169	8.41017	4.09 ns	M1+E2	263
Kr-83	9.4057	156.8 ns	M1+E2	17.09
Os-187	9.756	2.38 ns	M1(+E2)	280
U-235	13.0336	0.50 ns	(M1+E2)	497
Fe-57	14.4129	98.3 ns	M1+E2	8.56
Eu-151	21.541	9.6 ns	M1+E2	27.6
Sm-149	22.507	7.33 ns	M1+E2	29.2
Sn-119	23.870	18.03 ns	M1+E2	5.06
Hg-201	26.272	630 ps	M1+E2	71.6
K-40	29.8299	4.25 ns	M1	0.298
Hg-201	32.145	60 ps	M1+E2	39.6
Te-125	35.4925	1.482 ns	M1+E2	13.69
Os-189	36.17	0.52 ns	M1+E2	20.2
Sb-121	37.1298	3.46 ns	M1+E2	10.88
Xe-129	39.5774	0.97 ns	M1+E2	12.03
Dy-161	43.8201	0.83 ns	M1+E2	7.6
U-235	46.103	14 ps	M1+E2	50
W-183	46.4838	0.185 ns	M1+E2	8.4

which we have discussed previous in discussions of collimated X-ray emission. We note also the low-energy M1+E2 transition in ^{57}Fe at 14.4129 keV of interest in our excitation transfer experiments with radioactive ^{57}Co.

The calculation in the fourth-order indirect interactions discussed in this section involved a substantial effort, as on the order of a hundred pathways needed to be included, and as the resulting indirect coupling is extremely sensitive to any errors in the calculation. We had hoped that destructive interference effects might have been avoided for this model, but from the results we obtained it is clear that destructive interference very much impacts the indirect coupling leading to a very weak indirect interaction.

Even though there seems to be no hope accounting for the experimental results quantitatively with this model, there are some features of the model that are consistent qualitatively. In particular, we see excitation transfer dependent on the number of phonons present to nearest neighbors (in the case of phonon exchange with two phonon modes) which seems to be the kind of mechanism that would be relevant to observations of angular anisotropy. In addition we also see excitation transfer dependent on the number of phonons present potentially to distant neighbors (in the case of phonon exchange with one phonon mode) which seems to be what would be needed to account for delocalization effects observed in the experiments.

5. Loss

We found that loss can reduce the destructive interference that hinders the indirect coupling coefficient in the case of up-conversion and down-conversion [5,6]. Loss has the potential to similarly reduce the destructive interference in the case of excitation transfer. It was proposed a decade ago that the local environment can increase the excitation transfer rate in biophysics [17,18]. For phonon-mediated nuclear excitation transfer we have considered the simpler problem of the potential enhancement of the rate due to a difference in the loss for the different intermediate states.

5.1. Indirect coupling for lossy E1 excitation transfer

In the event that loss terms dominate the indirect coupling matrix element for E1 transitions we can write

$$\left(\hat{V}(E-\hat{H}_0)^{-1}\hat{V}\right)_{\rm resonant} \rightarrow$$
$$-i\frac{\hbar}{2}(\gamma_{00}+\gamma_{11}-\gamma_{01}-\gamma_{10})\frac{Mc^2}{2(\Delta E)^2}\sum_{j<j'}\sum_{m_0}\sum_{m_1}\sum_{m_0'}\sum_{m_1'}\left(|J_0m_0\rangle\langle J_1m_1|\right)_j\left(|J_1m_1'\rangle\langle J_0m_0'|\right)_{j'}$$
$$\langle J_0m_0|\mathbf{a}_j|J_1m_1\rangle\cdot\left[\frac{1}{N}\sum_{\mathbf{k},\sigma}(\hbar\omega_{\mathbf{k},\sigma})^2\mathbf{u}_{\mathbf{k},\sigma}\mathbf{u}_{\mathbf{k},\sigma}(2\hat{n}_{\mathbf{k},\sigma}+1)\cos\left(\mathbf{k}\cdot(\mathbf{R}_{j'}^{(0)}-\mathbf{R}_j^{(0)})\right)\right]\cdot\langle J_1m_1'|\mathbf{a}_{j'}|J_0m_0'\rangle$$
$$-i\frac{\hbar}{2}(\gamma_{00}+\gamma_{11}-\gamma_{01}-\gamma_{10})\frac{Mc^2}{2(\Delta E)^2}\sum_{j<j'}\sum_{m_0}\sum_{m_1}\sum_{m_0'}\sum_{m_1'}\left(|J_1m_1\rangle\langle J_0m_0|\right)_j\left(|J_0m_0'\rangle\langle J_1m_1'|\right)_{j'}$$
$$\langle J_1m_1|\mathbf{a}_j|J_0m_0\rangle\cdot\left[\frac{1}{N}\sum_{\mathbf{k},\sigma}(\hbar\omega_{\mathbf{k},\sigma})^2\mathbf{u}_{\mathbf{k},\sigma}\mathbf{u}_{\mathbf{k},\sigma}(2\hat{n}_{\mathbf{k},\sigma}+1)\cos\left(\mathbf{k}\cdot(\mathbf{R}_{j'}^{(0)}-\mathbf{R}_j^{(0)})\right)\right]\cdot\langle J_0m_0'|\mathbf{a}_{j'}|J_1m_1'\rangle\Big\}. \quad (35)$$

We have used a notation for the loss in which intermediate states where both nuclei in the ground state are assigned a loss of γ_{00}, intermediate states where both nuclei are in the excited state are assigned a loss of γ_{11}, and where the initial and final states are assigned a loss of γ_{10} and γ_{01} respectively. In the event that a small number of (delocalized) high-frequency phonon modes are very highly excited this version of the indirect interaction can be larger than the lossless contribution, and can be delocalized. This is interesting.

5.2. Loss for M1 transitions with two phonon modes

Instead of a recitation of all of the different terms for all of the different cases for nuclear excitation transfer for M1 transitions, we focus on one example. In the event that the loss terms dominate the resonant indirect interaction we can write

$$\left(\hat{V}(E-\hat{H}_0)^{-1}\hat{V}(E-\hat{H}_0)^{-1}\hat{V}(E-\hat{H}_0)^{-1}\hat{V}\right)_{\rm resonant} \rightarrow T_a+T_b \quad (36)$$

with

$$T_a=-i\frac{\hbar}{2}\frac{(Mc^2)^2}{4}\sum_{J_2}\sum_{J_2'}\Bigg\{\frac{\gamma_{01}-\gamma_{02'}-\gamma_{11}+\gamma_{12'}}{(E_1-E_0)(E_2'-E_0)(E_2-E_1)(E_2'-E_1)}$$
$$+\frac{\gamma_{00}-2\gamma_{01}+\gamma_{11}}{(E_1-E_0)^2(E_2-E_1)(E_2'-E_1)}+\frac{\gamma_{11}-\gamma_{12}-\gamma_{12'}+\gamma_{22'}}{(E_2-E_0)(E_2'-E_0)(E_2-E_1)(E_2'-E_1)}$$
$$+\frac{\gamma_{01}-\gamma_{02}-\gamma_{11}+\gamma_{12}}{(E_1-E_0)(E_2-E_0)(E_2-E_1)(E_2'-E_1)}\Bigg\}$$
$$\sum_j\sum_{j'}\sum_{m_0}\sum_{m_1}\sum_{m_2}\sum_{m_0'}\sum_{m_1'}\sum_{m_2'}\left(|J_0m_0\rangle\langle J_1m_1|\right)_j\left(|J_1m_1'\rangle\langle J_0m_0'|\right)_{j'}$$
$$\langle J_0m_0|\mathbf{a}_j|J_2m_2\rangle\cdot\left[\frac{1}{N}\sum_{\mathbf{k},\sigma}\hbar\omega_{\mathbf{k},\sigma}\mathbf{u}_{\mathbf{k},\sigma}\mathbf{u}_{\mathbf{k},\sigma}(2\hat{n}_{\mathbf{k},\sigma}+1)\cos\left(\mathbf{k}\cdot(\mathbf{R}_{j'}^{(0)}-\mathbf{R}_j^{(0)})\right)\right]\cdot\langle J_1m_1'|\mathbf{a}_{j'}|J_2'm_2'\rangle$$

$$\langle J_2 m_2|\mathbf{a}_j|J_1 m_1\rangle \cdot \left[\frac{1}{N}\sum_{\mathbf{k}',\sigma'}\hbar\omega_{\mathbf{k}',\sigma'}\mathbf{u}_{\mathbf{k}',\sigma'}\mathbf{u}_{\mathbf{k}',\sigma'}(2\hat{n}_{\mathbf{k}',\sigma}+1)\cos\left(\mathbf{k}'\cdot(\mathbf{R}^{(0)}_{j'}-\mathbf{R}^{(0)}_{j})\right)\right]\cdot\langle J'_2 m'_2|\mathbf{a}_{j'}|J_0 m'_0\rangle \tag{37}$$

$$T_b = -i\frac{\hbar}{2}\frac{(Mc^2)^2}{4}\sum_{J_2}\sum_{J'_2}\left\{\frac{\gamma_{01}-\gamma_{02'}-\gamma_{11}+\gamma_{12'}}{(E_1-E_0)(E'_2-E_0)(E_2-E_1)(E'_2-E_1)}\right.$$

$$+\frac{\gamma_{00}-2\gamma_{01}+\gamma_{11}}{(E_1-E_0)^2(E_2-E_1)(E'_2-E_1)}+\frac{\gamma_{11}-\gamma_{12}-\gamma_{12'}+\gamma_{22'}}{(E_2-E_0)(E'_2-E_0)(E_2-E_1)(E'_2-E_1)}$$

$$\left.+\frac{\gamma_{01}-\gamma_{02}-\gamma_{11}+\gamma_{12}}{(E_1-E_0)(E_2-E_0)(E_2-E_1)(E'_2-E_1)}\right\}$$

$$\sum_j\sum_{j'}\sum_{m_0}\sum_{m_1}\sum_{m_2}\sum_{m'_0}\sum_{m'_1}\sum_{m'_2}\left(|J_0 m_0\rangle\langle J_1 m_1|\right)_j\left(|J_1 m'_1\rangle\langle J_0 m'_0|\right)_{j'}$$

$$\langle J_0 m_0|\mathbf{a}_j|J_2 m_2\rangle\cdot\left[\frac{1}{N}\sum_{\mathbf{k},\sigma}\hbar\omega_{\mathbf{k},\sigma}\mathbf{u}_{\mathbf{k},\sigma}\mathbf{u}_{\mathbf{k},\sigma}(2\hat{n}_{\mathbf{k},\sigma}+1)\cos\left(\mathbf{k}\cdot(\mathbf{R}^{(0)}_{j'}-\mathbf{R}^{(0)}_{j})\right)\right]\cdot\langle J'_2 m'_2|\mathbf{a}_{j'}|J_0 m'_0\rangle$$

$$\langle J_2 m_2|\mathbf{a}_j|J_1 m_1\rangle\cdot\left[\frac{1}{N}\sum_{\mathbf{k}',\sigma'}\hbar\omega_{\mathbf{k}',\sigma'}\mathbf{u}_{\mathbf{k}',\sigma'}\mathbf{u}_{\mathbf{k}',\sigma'}(2\hat{n}_{\mathbf{k}',\sigma}+1)\cos\left(\mathbf{k}'\cdot(\mathbf{R}^{(0)}_{j'}-\mathbf{R}^{(0)}_{j})\right)\right]\cdot\langle J_1 m'_1|\mathbf{a}_{j'}|J'_2 m'_2\rangle \tag{38}$$

In writing this we have used the notation that the loss associated with basis states with two nuclei in the ground state is γ_{00}, the loss for basis states with one nucleus in the ground state and one in the first excited state is γ_{01}, and so forth.

Note that it is possible for contributions of this kind to be delocalized given a suitable distribution of phonons, and that that excitation can potentially be transferred to a great many nearby ground state nuclei.

5.3. Discussion

In order for loss to have a significant impact on the indirect coupling matrix element in the case of up-conversion and down-conversion there only needs to be a minor contribution associated with each phonon exchange, since a large number of phonon exchange interactions are involved. The situation is different in the case of excitation transfer. Since only a few phonon exchanges occur, the loss needs to be substantial in each case to have a significant impact on the overall indirect interaction.

Loss has the potential to greatly enhance excitation transfer based on the results discussed in this section. The indirect coupling coefficient are smaller than contributions from individual pathways by factors on the order of a differential decay rate times $\hbar$ divided by a relevant nuclear transition energy, which means that the terms are "small". However, if the number of phonons is large in a phonon mode that is delocalized, then the coupling from one site can be to a great many sites, which can increase the total coherent rate by a Dicke factor which is on the order of the square root of the number of possible final state sites.

It is possible that the excitation transfer effects we see in experiments with ^{57}Co are a result of loss-enhanced excitation transfer, but we would expect the differential decay rates not to be particularly large which argues against this. Nevertheless, in such a scenario we would only expect to see excitation transfer effects due to the presence of very highly-excited delocalized THz phonon modes.

6. Off-resonant Shift of the Basis State Energies

Although we found that loss could make a difference in the indirect interaction for excitation transfer in the previous section, the resulting indirect interaction seems too weak to account for the experimental results obtained so far.

Consequently, we are motivated to seek other effects that might impact the indirect interaction. One possibility which we discuss in this section is that the basis state energies may shift off of resonance, which could spoil the destructive interference if the shifts are sufficiently large.

That such an effect is possible in principle can be seen from the equivalent two-level system model of Eq. (11), where the basis state energies acquire a self-energy shift

$$E_n \;\rightarrow\; E_n + \Sigma(E), \tag{39}$$

where the self-energy $\Sigma(E)$ depends explicitly on the energy eigenvalue. If the self-energy depends on the energy eigenvalue, then its contribution would be different on resonance as compared to off-resonance.

We will argue in this section that there could well be a substantial shift in the basis state energies off of resonance. The main argument for this is that the nuclear force itself is due to the exchange of mesons, and since this exchange involves virtual states, the nuclear force is expected to depend on the energy eigenvalue. We would expect the binding energy of a nucleus to be different on resonance compared to off-resonance. In the literature there appears discussions in the 1960s and 1970s that the nucleon-nucleon interaction changes off of resonance, and that this would impact the calculation of various matrix elements contribute off of resonance, providing a constraint on nuclear potential models [19,20]. It would follow that the binding energy itself should differ off of resonance; however, there are no calculations of how the binding energy varies with the amount of energy off of resonance (most relevant may be the calculations discussed in Ref. [21]).

6.1. Brillouin–Wigner theory approach

We are interested in this subsection in applying Brillouin–Wigner theory to the problem of the off-resonant energy shift to a develop formalism to describe the effect. We consider a formal model given by

$$\hat{H} = \hat{H}_0 + \hat{U} + \hat{V}, \tag{40}$$

where $\hat{U}$ describes nuclear state raising and lowering associated with phonon exchange, and where $\hat{V}$ creates or destroys mesons in connection with the strong force.

We consider a sector expansion of the form

$$\begin{aligned}\Psi =& \Psi_{m,0} + \Psi_{m,1} + \cdots \\ &+ \Psi_{m-1,0} + \Psi_{m-1,1} + \cdots \\ &+ \Psi_{m+1,0} + \Psi_{m+1,1} + \cdots \\ &+ \cdots ,\end{aligned} \tag{41}$$

where the first index m keeps track of the number of excited nuclei present as a result of phonon exchange, and the second index is the number of mesons present associated with the nucleon-nucleon interaction. Keep in mind that we are considering the phonon exchange to be associated with phonon-nuclear coupling, so that a single phonon exchange is associated with the raising or lowering of the nuclear state. We plug in to the time-independent Schrödinger equation

$$E\Psi = \hat{H}\Psi \tag{42}$$

to obtain coupled eigenvalue equations given by

$$E\Psi_{m,0} = \hat{H}_0\Psi_{m,0} + \hat{U}_+\Psi_{m-1,0} + \hat{U}_-\Psi_{m+1,0} + \hat{V}_-\Psi_{m,1},$$

$$E\Psi_{m,1} = \hat{H}_0\Psi_{m,1} + \hat{U}_+\Psi_{m-1,1} + \hat{U}_-\Psi_{m+1,1} + \hat{V}_-\Psi_{m,2} + \hat{V}_+\Psi_{m,0},$$

$$E\Psi_{m-1,0} = \hat{H}_0\Psi_{m-1,0} + \hat{U}_+\Psi_{m-2,0} + \hat{U}_-\Psi_{m,0} + \hat{V}_-\Psi_{m-1,1},$$

$$E\Psi_{m-1,1} = \hat{H}_0\Psi_{m-1,1} + \hat{U}_+\Psi_{m-2,1} + \hat{U}_-\Psi_{m,1} + \hat{V}_-\Psi_{m-1,2} + \hat{V}_+\Psi_{m-1,0},$$

$$E\Psi_{m+1,0} = \hat{H}_0\Psi_{m+1,0} + \hat{U}_+\Psi_{m,0} + \hat{U}_-\Psi_{m+2,0} + \hat{V}_-\Psi_{m+1,1},$$

$$E\Psi_{m+1,1} = \hat{H}_0\Psi_{m+1,1} + \hat{U}_+\Psi_{m,1} + \hat{U}_-\Psi_{m+2,1} + \hat{V}_-\Psi_{m+1,2} + \hat{V}_+\Psi_{m+1,0},$$

$$\cdots \tag{43}$$

where we have made us of $\pm$ subscripts to keep track of raising or lowering.

For simplicity we would like to eliminate all sectors containing mesons in order to develop sector equations in terms of nuclear potential models. For simplicity our focus will be on single meson exchange, so that we need to eliminate all $\Psi_{m',1}$. To do this we first need to solve for these sector wave functions in terms of other sector wave functions according to

$$\Psi_{m,1} = (E - \hat{H}_0)^{-1}\left(\hat{U}_+\Psi_{m-1,1} + \hat{U}_-\Psi_{m+1,1} + \hat{V}_-\Psi_{m,2} + \hat{V}_+\Psi_{m,0}\right),$$

$$\Psi_{m-1,1} = (E - \hat{H}_0)^{-1}\left(\hat{U}_+\Psi_{m-2,1} + \hat{U}_-\Psi_{m,1} + \hat{V}_-\Psi_{m-1,2} + \hat{V}_+\Psi_{m-1,0}\right),$$

$$\Psi_{m+1,1} = (E - \hat{H}_0)^{-1}\left(\hat{U}_+\Psi_{m,1} + \hat{U}_-\Psi_{m+2,1} + \hat{V}_-\Psi_{m+1,2} + \hat{V}_+\Psi_{m+1,0}\right). \tag{44}$$

We plug in and retain only lowest order terms to obtain

$$E\Psi_{m,0} = \left(\hat{H}_0 + \hat{V}_-(E - \hat{H}_0)^{-1}\hat{V}_+\right)\Psi_{m,0} + \hat{U}_+\Psi_{m-1,0} + \hat{U}_-\Psi_{m+1,0},$$

$$E\Psi_{m-1,0} = \left(\hat{H}_0 + \hat{V}_-(E - \hat{H}_0)^{-1}\hat{V}_+\right)\Psi_{m-1,0} + \hat{U}_+\Psi_{m-2,0} + \hat{U}_-\Psi_{m,0},$$

$$E\Psi_{m+1,0} = \left(\hat{H}_0 + \hat{V}_-(E - \hat{H}_0)^{-1}\hat{V}_+\right)\Psi_{m+1,0} + \hat{U}_+\Psi_{m,0} + \hat{U}_-\Psi_{m+2,0},$$

$$\cdots \tag{45}$$

The single meson exchange contribution to the nucleon-nucleon potential on resonance in this simple model comes about through second-order terms of the form

$$\hat{V}_-(E-\hat{H}_0)^{-1}\hat{V}_+ \rightarrow \sum_{j<k}\frac{1}{3}\frac{g^2}{\hbar c}m_\pi c^2(\boldsymbol{\tau}_j\cdot\boldsymbol{\tau}_k)\left[\boldsymbol{\sigma}_j\cdot\boldsymbol{\sigma}_k+\left(1+\frac{3\hbar}{m_\pi c r_{jk}}+\frac{3\hbar^2}{m_\pi^2c^2r_{jk}^2}\right)S_{12}\right]\mathrm{e}^{-m_\pi c r_{jk}/\hbar}, \tag{46}$$

where we have selected here the one pion exchange potential from Ref. [22] for the resulting contribution to the nuclear potential. Note that in these older models that heavier meson exchange terms are included, and two-meson exchange terms are needed in order to develop a realistic potential model.

The key issue in this discussion is whether there is a shift in the binding energy due to a modification of the nucleon–nucleon potential off of resonance. To proceed, we first focus on the resonant sector where the energy eigenvalue is determined approximately from the solution of the formal eigenvalue equation

$$E\Psi_{m,0}=\left(\hat{H}_0+\hat{V}_-(E-\hat{H}_0)^{-1}\hat{V}_+\right)\Psi_{m,0}, \tag{47}$$

where the energy E in this equation appears both as the eigenvalue on the left-hand side and as part of the denominator on the right-hand side.

Consider next a similar calculation for the basis state energy in one of the off-resonant sectors. In this case we could work with the eigenvalue problem

$$E'\Psi_{m+1,0}=\left(\hat{H}_0+\hat{V}_-(E-\hat{H}_0)^{-1}\hat{V}_+\right)\Psi_{m+1,0}, \tag{48}$$

where E' is the associated eigenvalue, different from E by about one unit of excitation energy ΔE (since we consider $m+1$ instead of m). Suppose that for the purpose of sorting out the denominator on the right-hand side we approximate

$$E' \rightarrow E+\Delta E, \tag{49}$$

then we can write the eigenvalue equation for this off-resonant sector approximately as

$$E'\Psi_{m+1,0}=\left(\hat{H}_0+\hat{V}_-(E'-\Delta E-\hat{H}_0)^{-1}\hat{V}_+\right)\Psi_{m+1,0}. \tag{50}$$

The nuclear potential off of resonance will then be different than on resonance.

We can make use of a Taylor series expansion to determine the different in the nuclear potential at lowest order. We can write

$$(E'-\Delta E-\hat{H}_0)^{-1}=(E'-\hat{H}_0)^{-1}+\Delta E(E'-\hat{H}_0)^{-2}+\cdots \tag{51}$$

The off-resonance eigenvalue equation can be written approximately as

$$E'\Psi_{m+1,0}=\left(\hat{H}_0+\hat{V}_-(E'-\hat{H}_0)^{-1}\hat{V}_++\Delta E\hat{V}_-(E'-\hat{H}_0)^{-2}\hat{V}_+\right)\Psi_{m+1,0}. \tag{52}$$

To lowest order we would expect a shift in the binding energy linear in the offset energy

$$E' \;\rightarrow\; E + \Delta E + \Delta E \langle \hat{V}_- (E' - \hat{H}_0)^{-2} \hat{V}_+ \rangle. \tag{53}$$

Our conclusion from this brief discussion is that we would expect the nuclear binding energy to shift off of resonance. Also, if the nucleon–nucleon interaction changes off of resonance, we would also expect that the nuclear states themselves would be changed.

6.2. Breit interaction off of resonance

The arguments above apply as well to the electromagnetic interaction which is simpler and more familiar, so we were motivated to develop a calculation of the electromagnetic potential off of resonance. This is technically simplest in the Coulomb gauge, where the contribution from transverse photon exchange gives rise to the Breit interaction.

Single transverse photon exchange leads to an interaction that can be split into two components according to

$$\hat{V}_{12} = \hat{V}_{\rm I} + \hat{V}_{\rm II}, \tag{54}$$

where the initial evaluation of the second-order interaction leads to

$$\hat{V}_{\rm I} = q_1 q_2 \sum_{\mathbf{k}} \frac{\hbar c^2}{2\omega_{\mathbf{k}} \epsilon_0 L^3} \frac{(\boldsymbol{\alpha}_1 \cdot \boldsymbol{\alpha}_2)}{(E_{\rm off} - \hbar\omega_{\mathbf{k}})} + q_1 q_2 \sum_{\mathbf{k}} \frac{\hbar c^2}{2\omega_{\mathbf{k}} \epsilon_0 L^3} \frac{(\boldsymbol{\alpha}_2 \cdot \boldsymbol{\alpha}_1)}{(E_{\rm off} - \hbar\omega_{\mathbf{k}})} e^{i\mathbf{k}\cdot(\mathbf{r}_2 - \mathbf{r}_1)}, \tag{55}$$

$$\hat{V}_{\rm II} = -q_1 q_2 \sum_{\mathbf{k}} \frac{\hbar c^2}{2\omega_{\mathbf{k}} \epsilon_0 L^3} \frac{(\boldsymbol{\alpha}_1 \cdot \hat{\mathbf{i}}_{\mathbf{k}})(\boldsymbol{\alpha}_2 \cdot \hat{\mathbf{i}}_{\mathbf{k}})}{(E_{\rm off} - \hbar\omega_{\mathbf{k}})} e^{-i\mathbf{k}\cdot(\mathbf{r}_2 - \mathbf{r}_1)} - q_1 q_2 \sum_{\mathbf{k}} \frac{\hbar c^2}{2\omega_{\mathbf{k}} \epsilon_0 L^3} \frac{(\boldsymbol{\alpha}_2 \cdot \hat{\mathbf{i}}_{\mathbf{k}})(\boldsymbol{\alpha}_1 \cdot \hat{\mathbf{i}}_{\mathbf{k}})}{(E_{\rm off} - \hbar\omega_{\mathbf{k}})} e^{i\mathbf{k}\cdot(\mathbf{r}_2 - \mathbf{r}_1)}, \tag{56}$$

where $E_{\rm off}$ is the off-resonant shift in energy (for the off-resonant sector focused on in the previous section with one extra excited nucleus, $E_{\rm off} = -\Delta E$). These can be reduced in the continuum limit to give

$$\hat{V}_{\rm I} = -\frac{q_1 q_2}{4\pi\epsilon_0 |\mathbf{r}_2 - \mathbf{r}_1|} (\boldsymbol{\alpha}_1 \cdot \boldsymbol{\alpha}_2) \frac{2}{\pi} \int_0^\infty \frac{\sin(k|\mathbf{r}_2 - \mathbf{r}_1|)}{(k - E_{\rm off}/\hbar c)} {\rm d}k, \tag{57}$$

$$\begin{aligned} \hat{V}_{\rm II} =& \frac{q_1 q_2}{4\pi\epsilon_0} \frac{\boldsymbol{\alpha}_1 \cdot \boldsymbol{\alpha}_2}{3} \frac{2}{\pi} \int_0^\infty \frac{k j_0(k|\mathbf{r}_2 - \mathbf{r}_1|)}{(k - E_{\rm off}/\hbar c)} {\rm d}k \\ & - \frac{q_1 q_2}{4\pi\epsilon_0} \left((\boldsymbol{\alpha}_1 \cdot \hat{\mathbf{i}}_{\mathbf{r}_2 - \mathbf{r}_1})(\boldsymbol{\alpha}_2 \cdot \hat{\mathbf{i}}_{\mathbf{r}_2 - \mathbf{r}_1}) - \frac{\boldsymbol{\alpha}_1 \cdot \boldsymbol{\alpha}_2}{3} \right) \frac{2}{\pi} \int_0^\infty \frac{k j_2(k|\mathbf{r}_2 - \mathbf{r}_1|)}{(k - E_{\rm off}/\hbar c)} {\rm d}k. \end{aligned} \tag{58}$$

On resonance these reduce to

$$\begin{aligned} \hat{V}_{\rm I} + \hat{V}_{\rm II} =& -\frac{q_1 q_2}{4\pi\epsilon_0 |\mathbf{r}_2 - \mathbf{r}_1|} (\boldsymbol{\alpha}_1 \cdot \boldsymbol{\alpha}_2) \\ & + \frac{q_1 q_2}{4\pi\epsilon_0 |\mathbf{r}_2 - \mathbf{r}_1|} \frac{\boldsymbol{\alpha}_1 \cdot \boldsymbol{\alpha}_2}{3} - \frac{q_1 q_2}{4\pi\epsilon_0 |\mathbf{r}_2 - \mathbf{r}_1|} \frac{1}{2} \left((\boldsymbol{\alpha}_1 \cdot \hat{\mathbf{i}}_{\mathbf{r}_2 - \mathbf{r}_1})(\boldsymbol{\alpha}_2 \cdot \hat{\mathbf{i}}_{\mathbf{r}_2 - \mathbf{r}_1}) - \frac{\boldsymbol{\alpha}_1 \cdot \boldsymbol{\alpha}_2}{3} \right) \\ =& -\frac{1}{2} \frac{q_1 q_2}{4\pi\epsilon_0 |\mathbf{r}_2 - \mathbf{r}_1|} \left[(\boldsymbol{\alpha}_1 \cdot \boldsymbol{\alpha}_2) + (\boldsymbol{\alpha}_1 \cdot \hat{\mathbf{i}}_{\mathbf{r}_2 - \mathbf{r}_1})(\boldsymbol{\alpha}_2 \cdot \hat{\mathbf{i}}_{\mathbf{r}_2 - \mathbf{r}_1}) \right] \end{aligned} \tag{59}$$

consistent with the Breit interaction found in the literature.

6.3. Pole on the integration contour

In the event that $E_{\rm off}$ is positive (so that the energy eigenvalue is larger than the basis state energy) then the integrals in k contain a pole on the k-axis in the range of integration. We can write [23]

$$\int_0^\infty \frac{\sin(k|\mathbf{r}_2-\mathbf{r}_1|)}{(k-k_0)}{\rm d}k$$
$$= -\sin(k_0|\mathbf{r}_2-\mathbf{r}_1|){\rm ci}(k_0|\mathbf{r}_2-\mathbf{r}_1|)+\cos(k_0|\mathbf{r}_2-\mathbf{r}_1|)[{\rm si}(k_0|\mathbf{r}_2-\mathbf{r}_1|)+\pi], \tag{60}$$

where

$$k_0 = \frac{E_{off}}{\hbar c}, \tag{61}$$

$${\rm si}(a) = -\int_1^\infty \frac{\sin(ax)}{x}{\rm d}x,$$

$${\rm ci}(a) = -\int_1^\infty \frac{\cos(ax)}{x}\,{\rm d}x. \tag{62}$$

The pole on the k-axis in this case does not lead to an imaginary contribution, so we would not expect a new radiative decay channel off of resonance resulting from this contribution.

For the other off-resonant integral

$$\int_0^\infty \frac{k}{k-k_0} j_2(k|\mathbf{r}_2-\mathbf{r}_1|){\rm d}k, \tag{63}$$

we can express the result in terms of the Meijer G-function when $k_0<0$. At present we do not have a result for the extension to $k_0>0$, so we do not know whether an imaginary part is generated.

6.4. Indirect interaction for E1 transitions

Under conditions where basis state energy shifts provide the dominant contribution to the indirect second order interaction for excitation transfer associated with E1 transitions we can write for the resonant interaction

$$\left(\hat{V}(E-\hat{H}_0)^{-1}\hat{V}\right)_{\rm resonant}$$
$$\rightarrow \sum_j\sum_{j'}\sum_{m_0}\sum_{m_1}\sum_{m_0'}\sum_{m_1'}\sum_{\mathbf{k},\sigma}\frac{Mc^2\hbar\omega_{\mathbf{k},\sigma}}{2N}$$
$$\Big\{|J_0m_0\rangle\langle J_0m_0|\mathbf{u}_{\mathbf{k},\sigma}\cdot\mathbf{a}_j|J_1m_1\rangle\langle J_1m_1||J_1m_1'\rangle\langle J_1m_1'|\mathbf{u}_{\mathbf{k},\sigma}\cdot\mathbf{a}_{j'}|J_0m_0'\rangle\langle J_0m_0'|$$
$$\frac{E_{00}+E_{11}-2E_{10}}{(E_{10}-E_{00})(E_{11}-E_{10})}(2\hat{n}_{\mathbf{k},\sigma}+1)\cos[\mathbf{k}\cdot(\mathbf{R}_{j'}^{(0)}-\mathbf{R}_j^{(0)})]$$
$$+|J_1m_1\rangle\langle J_1m_1|\mathbf{u}_{\mathbf{k},\sigma}\cdot\mathbf{a}_j|J_0m_0\rangle\langle J_0m_0||J_0m_0'\rangle\langle J_0m_0'|\mathbf{u}_{\mathbf{k},\sigma}\cdot\mathbf{a}_{j'}|J_1m_1'\rangle\langle J_1m_1'|$$
$$\frac{E_{00}+E_{11}-2E_{10}}{(E_{10}-E_{00})(E_{11}-E_{10})}(2\hat{n}_{\mathbf{k},\sigma}+1)\cos[\mathbf{k}\cdot(\mathbf{R}_{j'}^{(0)}-\mathbf{R}_j^{(0)})]\Big\}, \tag{64}$$

where E_{00} is the (shifted) basis state energy with both nuclei in the ground state, where E_{11} is the (shifted) basis state energy with both nuclei in the excited state, and where $E_{10} = E_{01}$ is the (unshifted) basis state energy with one nucleus excited and one in the ground state.

6.5. Indirect interaction for one-mode M1 transitions

The indirect interaction for resonant excitation transfer for an M1 transition involving exchange with a single phonon mode can be written as

$$\left(\hat{V}(E-\hat{H}_0)^{-1}\hat{V}(E-\hat{H}_0)^{-1}\hat{V}(E-\hat{H}_0)^{-1}\hat{V}\right)_{\rm resonant} \rightarrow T_{c0}+T_{c1}+T_{c2}+T_{s1}, \tag{65}$$

where

$$\begin{aligned}
T_{c0} =& \frac{(Mc^2)^2}{4N}\sum_{J_2}\sum_{J_2'}\left(\frac{2}{(E_{10}-E_{00})(E_{10}-E_{20})(E_{10}-E_{2'0})}+\frac{2}{(E_{10}-E_{11})(E_{10}-E_{21})(E_{10}-E_{2'1})}\right.\\
&\left.+\frac{1}{(E_{10}-E_{20})(E_{10}-E_{2'0})(E_{10}-E_{2'2})}+\frac{1}{(E_{10}-E_{21})(E_{10}-E_{2'1})(E_{10}-E_{2'2})}\right)\\
&\sum_j\sum_{j'}\sum_{m_0}\sum_{m_1}\sum_{m_2}\sum_{m_0'}\sum_{m_1'}\sum_{m_2'}\left(|J_0m_0\rangle\langle J_1m_1|\right)_j\left(|J_1m_1'\rangle\langle J_0m_0'|\right)_{j'}\\
&\sum_\alpha\sum_\beta\sum_\gamma\sum_\delta(\langle J_0m_0|\mathbf{a}_j|J_2m_2\rangle)_\alpha(\langle J_2m_2|\mathbf{a}_j|J_1m_1\rangle)_\beta(\langle J_1m_1'|\mathbf{a}_{j'}|J_2'm_2'\rangle)_\gamma(\langle J_2'm_2'|\mathbf{a}_{j'}|J_0m_0'\rangle)_\delta\\
&\left[\frac{1}{N}\sum_{\mathbf{k},\sigma}(\hbar\omega_{\mathbf{k},\sigma})^2(\mathbf{u}_{\mathbf{k},\sigma})_\alpha(\mathbf{u}_{\mathbf{k},\sigma})_\beta(\mathbf{u}_{\mathbf{k},\sigma})_\gamma(\mathbf{u}_{\mathbf{k},\sigma})_\delta\cos\left(2\mathbf{k}(\mathbf{R}_{j'}^{(0)}-\mathbf{R}_j^{(0)})\right)\right]
\end{aligned} \tag{66}$$

$$\begin{aligned}
T_{c1} =& \frac{(Mc^2)^2}{4N}\sum_{J_2}\sum_{J_2'}\left(\frac{2}{(E_{10}-E_{00})(E_{10}-E_{20})(E_{10}-E_{2'0})}+\frac{2}{(E_{10}-E_{11})(E_{10}-E_{21})(E_{10}-E_{2'1})}\right.\\
&+\frac{2}{(E_{10}-E_{20})(E_{10}-E_{21})(E_{10}-E_{2'2})}+\frac{2}{(E_{10}-E_{20})(E_{10}-E_{2'0})(E_{10}-E_{2'2})}\\
&\left.+\frac{2}{(E_{10}-E_{21})(E_{10}-E_{2'0})(E_{10}-E_{2'2})}+\frac{2}{(E_{10}-E_{2'0})(E_{10}-E_{2'1})(E_{10}-E_{2'2})}\right)\\
&\sum_j\sum_{j'}\sum_{m_0}\sum_{m_1}\sum_{m_2}\sum_{m_0'}\sum_{m_1'}\sum_{m_2'}\left(|J_0m_0\rangle\langle J_1m_1|\right)_j\left(|J_1m_1'\rangle\langle J_0m_0'|\right)_{j'}\\
&\sum_\alpha\sum_\beta\sum_\gamma\sum_\delta(\langle J_0m_0|\mathbf{a}_j|J_2m_2\rangle)_\alpha(\langle J_2m_2|\mathbf{a}_j|J_1m_1\rangle)_\beta(\langle J_1m_1'|\mathbf{a}_{j'}|J_2'm_2'\rangle)_\gamma(\langle J_2'm_2'|\mathbf{a}_{j'}|J_0m_0'\rangle)_\delta\\
&\left[\frac{1}{N}\sum_{\mathbf{k},\sigma}(\hbar\omega_{\mathbf{k},\sigma})^2(\mathbf{u}_{\mathbf{k},\sigma})_\alpha(\mathbf{u}_{\mathbf{k},\sigma})_\beta(\mathbf{u}_{\mathbf{k},\sigma})_\gamma(\mathbf{u}_{\mathbf{k},\sigma})_\delta\hat{n}_{\mathbf{k},\sigma}\cos\left(2\mathbf{k}(\mathbf{R}_{j'}^{(0)}-\mathbf{R}_j^{(0)})\right)\right]
\end{aligned} \tag{67}$$

$$T_{c2} = \frac{(Mc^2)^2}{4N} \sum_{J_2} \sum_{J_2'} \left(\frac{2}{(E_{10}-E_{00})(E_{10}-E_{20})(E_{10}-E_{2'0})} + \frac{2}{(E_{10}-E_{11})(E_{10}-E_{21})(E_{10}-E_{2'1})} \right.$$
$$+ \frac{2}{(E_{10}-E_{20})(E_{10}-E_{21})(E_{10}-E_{2'2})} + \frac{2}{(E_{10}-E_{20})(E_{10}-E_{2'0})(E_{10}-E_{2'2})}$$
$$\left. + \frac{2}{(E_{10}-E_{21})(E_{10}-E_{2'1})(E_{10}-E_{2'2})} + \frac{2}{(E_{10}-E_{2'0})(E_{10}-E_{2'1})(E_{10}-E_{2'2})} \right)$$
$$\sum_j \sum_{j'} \sum_{m_0} \sum_{m_1} \sum_{m_2} \sum_{m_0'} \sum_{m_1'} \sum_{m_2'} \left(|J_0 m_0\rangle\langle J_1 m_1| \right)_j \left(|J_1 m_1'\rangle\langle J_0 m_0'| \right)_{j'}$$
$$\sum_\alpha \sum_\beta \sum_\gamma \sum_\delta (\langle J_0 m_0 | \mathbf{a}_j | J_2 m_2 \rangle)_\alpha (\langle J_2 m_2 | \mathbf{a}_j | J_1 m_1 \rangle)_\beta (\langle J_1 m_1' | \mathbf{a}_{j'} | J_2' m_2' \rangle)_\gamma (\langle J_2' m_2' | \mathbf{a}_{j'} | J_0 m_0' \rangle)_\delta$$
$$\left[\frac{1}{N} \sum_{\mathbf{k},\sigma} (\hbar\omega_{\mathbf{k},\sigma})^2 (\mathbf{u}_{\mathbf{k},\sigma})_\alpha (\mathbf{u}_{\mathbf{k},\sigma})_\beta (\mathbf{u}_{\mathbf{k},\sigma})_\gamma (\mathbf{u}_{\mathbf{k},\sigma})_\delta \hat{n}_{\mathbf{k},\sigma}^2 \cos\left(2\mathbf{k}(\mathbf{R}_{j'}^{(0)} - \mathbf{R}_j^{(0)}) \right) \right], \tag{68}$$

$$T_{s1} = i\frac{(Mc^2)^2}{4N} \sum_{J_2} \sum_{J_2'} \left(\frac{2}{(E_{10}-\text{Eaa})(E_{10}-\text{Eca})(E_{10}-\text{Eda})} - \frac{2}{(E_{10}-\text{Ebb})(E_{10}-\text{Ecb})(E_{10}-\text{Edb})} \right.$$
$$\left. + \frac{1}{(E_{10}-\text{Eca})(E_{10}-\text{Eda})(E_{10}-\text{Edc})} - \frac{1}{(E_{10}-\text{Ecb})(E_{10}-\text{Edb})(E_{10}-\text{Edc})} \right)$$
$$\sum_j \sum_{j'} \sum_{m_0} \sum_{m_1} \sum_{m_2} \sum_{m_0'} \sum_{m_1'} \sum_{m_2'} \left(|J_0 m_0\rangle\langle J_1 m_1| \right)_j \left(|J_1 m_1'\rangle\langle J_0 m_0'| \right)_{j'}$$
$$\sum_\alpha \sum_\beta \sum_\gamma \sum_\delta (\langle J_0 m_0 | \mathbf{a}_j | J_2 m_2 \rangle)_\alpha (\langle J_2 m_2 | \mathbf{a}_j | J_1 m_1 \rangle)_\beta (\langle J_1 m_1' | \mathbf{a}_{j'} | J_2' m_2' \rangle)_\gamma (\langle J_2' m_2' | \mathbf{a}_{j'} | J_0 m_0' \rangle)_\delta$$
$$\left[\frac{1}{N} \sum_{\mathbf{k},\sigma} (\hbar\omega_{\mathbf{k},\sigma})^2 (\mathbf{u}_{\mathbf{k},\sigma})_\alpha (\mathbf{u}_{\mathbf{k},\sigma})_\beta (\mathbf{u}_{\mathbf{k},\sigma})_\gamma (\mathbf{u}_{\mathbf{k},\sigma})_\delta \hat{n}_{\mathbf{k},\sigma} \sin\left(2\mathbf{k}(\mathbf{R}_{j'}^{(0)} - \mathbf{R}_j^{(0)}) \right) \right]. \tag{69}$$

In this case the only destructive interference comes from the symmetry of the Brillouin zone for a term proportional to $\sin\left(2\mathbf{k}(\mathbf{R}_{j'}^{(0)} - \mathbf{R}_j^{(0)}) \right)$ that is independent of the number of phonons present. In this model we have a candidate mechanism with a good chance of connecting with our experiments, as long as the off resonant shift of the basis state energies is substantial.

6.6. Discussion

We have as yet not worked out off-resonant nuclear potential models, although this is currently at the top of our list of projects to address. Were we to focus on the older meson exchange models (Hamada–Johnston potential [24], Reid potential [25], Argonne potential [26], etc.), then it might be possible to develop off-resonant extensions of individual terms that appear in the models based on arguments about the interactions involved and the number of mesons exchanged. However, since the older models are empirical this kind of extension comes with issues associated with the extension. If we focus on the newer chiral effective field theory models [27,28], then the proposed extension is much simpler (at least at low order) and better defined since the chiral effective field theory model itself is simpler.

It would be possible to augment our relativistic Dirac–Fock code to evaluate electronic shifts off of resonance based on the off-resonant version of the Breit interaction in this section.

The indirect interactions for models with off-resonant shifts of the basis state energies are impacted by destructive interference effects much less if the shifts are large (much greater than the maximum phonon energy). We have given the interaction for the M1

single mode case, and the other cases with two modes and three modes behave similarly. These models have the best chance of being able to account for our experimental results, and will be the focus of our studies in the near future.

Note that a shift of the basis state energies off of resonance would have the potential to greatly increase the indirect coupling matrix element associated with up-conversion and down-conversion.

7. Issues Raised in the ^{57}Co Experiments

As mentioned above in May 2017 we observed non-exponential decay effects in experiments where radioactive ^{57}Co was evaporated on a steel sample and mechanical stress was applied [10]. In subsequent experiments we have sought to develop an understanding, and in the process a number of issues have emerged. In this section we focus on a subset of the issues.

7.1. Angular anisotropy

We see in Fig. 1 that following the beta decay of ^{57}Co that the 136.5 keV state of ^{57}Fe is populated, resulting in energetic gammas at 136.5 keV and at 122.1 keV. We have seen non-exponential decay effects associated with these lines [10,13], which we have interpreted as due to a (dynamic) angular anisotropy resulting from resonant excitation transfer.

In the simplest possible relevant excitation transfer model, we consider an excited state ^{57}Fe nucleus in a local BCC lattice made up of ^{57}Fe nuclei (corresponding to a simplistic picture of the residue on the surface of the steel). In a model with excitation transfer only to the eight nearest neighbors, the maximum probability amplitude $c_{\rm max}$ at the nearest neighbors satisfies

$$\sqrt{8}|c_{\rm max}| = \sqrt{8}\frac{2|V_{\rm indirect}|}{\hbar\gamma}, \tag{70}$$

where $V_{\rm indirect}$ is the indirect coupling matrix element from the initial excited ^{57}Fe nucleus to a nearest neighbor, and where γ is the decay rate of the excitation. A dynamical model for the simpler two-site case is described in Appendix B. To be consistent with the experimental results, we would need for $\sqrt{8}|c_{\rm max}|$ to be on the order of 0.1 or so, from which we might estimate the indirect coupling matrix element to be on the order of

$$|V_{\rm indirect}| \;\rightarrow\; \frac{1}{2}\,0.1\,\hbar\gamma = 1.6\times10^{-8}\ {\rm eV}. \tag{71}$$

The associated theoretical problem is that generally the estimates from the models described in the previous sections lead to indirect coupling matrix elements that are much smaller than this. The thought is that models based on the shift in basis state energies off of resonance probably have the best chance of achieving consistency, but much work remains to develop a reliable estimate from the models.

7.2. Variation of the incremental 14.4 keV gamma to Fe K$_\alpha$ ratio

In the first observation of non-exponential decay effects in May 2017 we saw a roughly 19% increase in the 14.4 keV emission, and a roughly 17% increase in the Fe K$_\alpha$ emission [10]. In subsequent experiments we have seen different incremental ratios: in some cases the incremental 14.4 keV gamma intensity was greater than 19/17 times the incremental Fe K$_\alpha$ X-ray intensity, and in other cases the incremental Fe K$_\alpha$ intensity was more than twice the incremental 14.4 keV gamma intensity. Air absorption causes a reduction the lower energy Fe K$_\alpha$ X-ray intensity, and when using a thermal pulse for stimulation the air absorption is reduced a small amount, which complicates the analysis of the data. Nevertheless, it appears that this incremental ratio is showing an unexpected variation in our experiments, and that this effect may be important.

One potential route toward an explanation is to note that in perturbation theory there are new decay channels available in which the energy from one 14.4 keV excitation can be dissipated at two sites through two internal conversion processes in some of the off-resonant states producing two K-shell holes instead of one. This can lead to an increase in the incremental Fe K$_\alpha$ intensity relative to the incremental 14.4 keV gamma intensity. Some discussion of internal conversion in connection with excitation transfer is given in Appendix C.

7.3. Changes in the 14.4 keV gamma intensity

In January 2018 an experiment was done with our Sample 2 in which a thermal pulse was used to create incremental mechanical stress, and an X-ray detector monitored emission from all of the evaporated region with no mesh blocking the signal. In this case we saw a decrease in the 14.4 keV intensity. This observation permits an interpretation that some of the excitation is transferring into the steel so that the subsequent gamma emission is absorbed.

In late Spring 2018 we carried out a version of this experiment with our Sample 1, hoping to see a similar result. Instead we saw an increase in the 14.4 keV gamma intensity [13]. The difference in the results tells us that the two samples behave very differently, a conclusion that is consistent with many other experiments (our Sample 2 in general tends not to do very much for us). In other experiments where a mesh or pinhole was used, we had been thinking that a delocalization of the excitation could account for an increase or decrease in intensity. However, for these experiments no mesh or pinhole was used.

It might be argued that angular anisotropy might play some role for the 14.4 keV transition; however, in other experiments we have not seen much evidence for angular anisotropy on this line. In both cases there is a qualitatively similar response of the Fe K_α, which cannot show angular anisotropy.

In upcoming experiments we need to use the HPGe detector to monitor the harder gammas at the same time as the 14.4 keV line to clarify whether we might be seeing a subdivision effect (in which the excitation of the 136.5 keV state is divided between several 14.4 keV states, with the dissipation of the left over energy).

7.4. Coincidence measurements

In previous years when we were studying models for up-conversion and for down-conversion, we found that the coupled quantum system seemed to avoid the occupation of states which decayed rapidly, and seemed to favor states with no open decay channels. The conclusion was that in this kind of system one would expect a net reduction in the decay rate over what might be expected if this effect did not occur. In these models we assumed that decay channels would generally be closed for basis states far off of resonance where the basis state energy exceeded the energy eigenvalue.

If we are seeing changes in the incremental 14.4 keV to Fe K_α ratio, then it is possible that this indicates significant occupation of off-resonance states. If so, then it may be that the decay channels are closed for some of the off-resonant states. Consequently we are motivated to consider coincidence experiments in which we monitor to see whether the 14.4 keV gamma arrives within a window of 100 ns or so following the initial beta decay of the ^{57}Co. A coincidence experiment with a properly set acceptance window has the potential to address this issue.

The beta decay of the ^{57}Co occurs with the absorption of a K-shell electron, leaving a K-shell hole in the newly formed ^{57}Fe daughter. Consequently, some of the time we will get a prompt Fe K_α that could be used to trigger the start of an acceptance window in time. The half-life of the 136.5 keV state is 8.7 ns, so that we could instead make use of the 122.1 keV gamma for triggering. In either case a time window near 100 ns would get most of the 14.4 keV emission (the half-life of the 14.4 keV state is 98.3 ns). If the rate of 14.4 keV gammas detected in this window were to drop with mechanical stimulation, and if the rate of 14.4 keV gammas arriving later were to correspondingly increase, then this could indicate that the half-life of the 14.4 keV state was increased. We are considering an experiment of this kind in the coming months.

7.5. Delocalization

Lu took pinhole camera images of the ^{57}Co residue, which showed that the emission was strongest in a ring around the edge of the residue with a "hot spot" evident where the ^{57}Co had collected preferentially [13]. In subsequent experiments with a pinhole and Amptek SDD X-ray detector, the time history of different parts of the ring and hot spot were monitored during thermal stimulation under stress. In the vicinity of the "hot spot" we saw the largest increase in intensity for the 14.4 keV gamma and for the Fe K_α X-ray. In other places we saw lesser increases, and in one location distant from the "hot spot" we saw a decrease in emission. These observations permit an interpretation of a delocalization of the excitation in the residue [13]. In connection with these experiments we have proposed that our radioactive ^{57}Co source contains much ^{57}Fe, and that the residue observed in optical photographs is primarily ^{57}Fe on the surface of the steel (this was suggested by Malcolm Fowler).

This observation focuses our attention on fourth-order indirect interactions for excitation transfer where the interaction can be delocalized.

8. Possibility of E1 Excitation Transfer Experiments

As discussed above, excitation transfer for E1 transitions is accounted for in perturbation theory through a second-order interaction, while excitation transfer for M1 transitions appears as a fourth-order interaction. Note that we would expect a fourth-order interaction in general to be much weaker than a second-order interaction when the coupling is weak. In our excitation transfer experiments with a ^{57}Co source on steel we have seen striking unexpected non-exponential decay effects, involving primarily M1 transitions for the 14.4 keV state and for the 136.5 keV state. This provides motivation for pursuing excitation transfer studies with E1 transitions, which may show a stronger version of the effects.

8.1. Radioactive sources

To develop an analogous excitation transfer experiment for an E1 transition, the big issue has to do with the procurement of a relevant radioactive source. The low energy E1 transitions and potential source isotopes are listed in Table 3. The most interesting candidate E1 transition is the 6.237 keV transition in ^{181}Ta, for which potential sources might be ^{181}Hf and ^{181}W, where ^{181}W is the better choice as it is more efficient in populating the 6.237 keV state. Unfortunately it does not seem possible to obtain ^{181}W from a supplier at this time.

Table 3. Radioactive sources that might be used to produce excited states for E1 transitions.

Isotope	E(keV)	Source (Z-1)	Half-life	Source (Z+1)	Half-life
Ta-181	6.237	Hf-181	42.4 d	W-181	121 d
Dy-161	25.65135	Tb-161	6.90 d	Ho-161	2.48 h
Gd-157	63.929	Eu-157	15.13 h	Tb-157	150 y
Dy-161	74.56668	Tb-161	6.90 d	Ho-161	2.48 h
Gd-155	86.5479	Eu-155	4.9 y	Tb-155	5.3 d
Eu-153	97.43100	Sm-153	46.8 h	Gd-153	241.6 d
Dy-161	103.062	Tb-161	6.90 d	Ho-161	2.48 h
Gd-155	105.3083	Eu-155	4.9 y	Tb-155	5.3 d
F-19	109.9	O-19	26.9 s	Ne-19	17.3 s
Dy-161	131.8	Tb-161	6.90 d	Ho-161	2.48 h
Eu-153	151.6245	Sm-153	46.8 h	Gd-153	241.6 d

The half-life for sources with mass 161 are too short to be useful. At mass 157 we see ^{157}Tb with a long half-life, but when it decays to ^{157}Gd very little (0.34%) population of the 63.9 keV excited state occurs. For mass 155 we see ^{155}Eu with a 4.9 year half-life, which appears to be available as a radioactive source from suppliers. The fraction of the decays that go directly to the 86.5 keV second excited state is 26%, which looks good. At mass 153 ^{153}Gd looks to have a usefully long half-life, the fraction of decays that go to the 97.3 keV state is 37%, and ^{153}Gd appears to be available as a radioactive source.

8.2. Nuclear Bragg scattering with resonant excitation transfer

For low-energy nuclear transitions for which no commercially available radioactive sources are available the question arises as to whether there is some other route to the detection of phonon-induced nuclear excitation transfer. Instead of populating nuclear excited states following beta decay, we might consider exciting them directly with narrow band synchrotron radiation. The use of narrow band radiation from synchrotron sources for applications involving low energy nuclear transitions is reviewed in Refs. [29–31]. A variety of experimental techniques have been pioneered to observe nuclear Bragg scattering, hyperfine effects from oscillations of the scattered signal, phonon interactions, diffusion, and a variety of other effects as well.

The question of interest here is whether resonant excitation transfer might be observed in a nuclear Bragg scattering experiment. Consider a simple model for the vector potential for the scattered wave in the far field which we might write as

$$\hat{A}_z(\mathbf{r}) \;\rightarrow\; -i\omega\frac{\mu_0}{4\pi|\mathbf{r}|}\,\mathrm{e}^{ikr}\sum_j d_j \mathrm{e}^{-i\mathbf{k}\cdot\mathbf{r}_j} \tag{72}$$

with scattered wave vector $\mathbf{k}$, assuming z-polarized incident light with the z-directed dipole moment d_j associated with nucleus j. For simple Bragg diffraction with no phonon exchange and no excitation transfer the induced dipole moments are phase dependent according to

$$d_j = d_0 \mathrm{e}^{i\mathbf{k}_0\cdot\mathbf{r}_j} \tag{73}$$

with incident wave vector $\mathbf{k}_0$. We might model resonant excitation transfer as involving a modification in which the nuclear dipole moment acquires contributions from coupling with other sites according to

$$d_j = d_0 \mathrm{e}^{i\mathbf{k}_0\cdot\mathbf{r}_j} + \sum_l d_{j,l}\,\mathrm{e}^{i\mathbf{k}_0\cdot\mathbf{r}_l}, \tag{74}$$

where $d_{j,l}$ accounts for the contribution to the nuclear dipole moment at site j due to resonant excitation transfer from site l. The phase factors associated with resonant excitation transfer in this model are consistent with the dynamical model discussed in Appendix B. In this case we can write for the ratio of the part of the diffracted intensity due to excitation transfer relative to the unperturbed diffracted intensity

$$\frac{\Delta I}{I} = \frac{\sum_{j,j',l} d^*_{j',l} d_0 \mathrm{e}^{i(\mathbf{k}_0-\mathbf{k})\cdot\mathbf{r}_j}\mathrm{e}^{-i\mathbf{k}_0\cdot\mathbf{r}_l}\mathrm{e}^{i\mathbf{k}\cdot\mathbf{r}_{j'}} + \sum_{j,j',l} d_{j',l} d^*_0 \mathrm{e}^{-i(\mathbf{k}_0-\mathbf{k})\cdot\mathbf{r}_j}\,\mathrm{e}^{i\mathbf{k}_0\cdot\mathbf{r}_l}\mathrm{e}^{-i\mathbf{k}\cdot\mathbf{r}_{j'}}}{|d_0|^2\sum_{j,j'}\mathrm{e}^{i(\mathbf{k}_0-\mathbf{k})\cdot(\mathbf{r}_j-\mathbf{r}_{j'})}}. \tag{75}$$

This can be rewritten in the form

$$\frac{\Delta I}{I} = \frac{\left[\sum_j D_j \mathrm{e}^{i(\mathbf{k}_0-\mathbf{k})\cdot\mathbf{r}_j}\right]^*}{d^*_0\left[\sum_j \mathrm{e}^{i(\mathbf{k}_0-\mathbf{k})\cdot\mathbf{r}_j}\right]^*} + \frac{\left[\sum_j D_j \mathrm{e}^{i(\mathbf{k}_0-\mathbf{k})\cdot\mathbf{r}_j}\right]}{d_0\left[\sum_j \mathrm{e}^{i(\mathbf{k}_0-\mathbf{k})\cdot\mathbf{r}_j}\right]}, \tag{76}$$

where we have defined the D_j according to

$$D_j = \sum_l d_{j,l}\mathrm{e}^{i\mathbf{k}_0\cdot(\mathbf{r}_l-\mathbf{r}_j)}. \tag{77}$$

The conclusion from this simple model is that resonant excitation transfer may be observable as a change in the intensity of the Bragg peaks.

It seems from the literature that the 14.4 keV transition in ^{57}Fe has been most studied, at least in the early experimental work. Given that our excitation transfer experiments have focused primarily on this transition, it would seem that if experiments as proposed here are pursued, they should probably focus first on establishing the existence of such an effect with the 14.4 keV transition. Afterward, similar experiments on other transitions would be of interest.

One of the most interesting non-iron candidates is the 6.237 keV transition in ^{181}Ta since it is the lowest energy accessible E1 transition, and has the potential to address numerous theoretical issues. The big headache with this transition is that it is normally very weak in Mössbauer experiments since radiative decay is much slower than internal conversion. Nevertheless, this transition has been studied with synchrotron radiation (see Refs. [32–34]). The energy of the line was determined in Ref. [32] to be 6.214 ± 2 keV, which is an improvement over previous determinations. We have used 6.237 keV in this paper consistent with the BNL Nudat2 database energy level, which has not been updated with this revised value.

9. Excitation Transfer from $D_2/^4$He and HD/^{3}He

One of our earliest proposals for excitation transfer in connection with experiments in Condensed Matter Nuclear Science [5] concerned a candidate explanation for low-level energetic alpha emission from thin film palladium deuterated through ion bombardment by Chambers et al. [35]. We proposed excitation transfer of a large 24 MeV quantum from the nuclear system $D_2/^4$He to a Pd

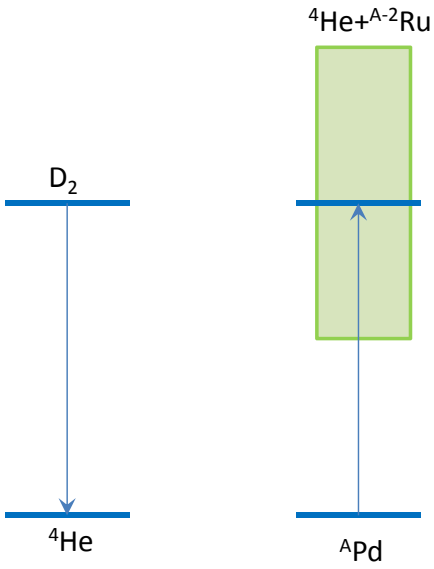

Figure 2. Excitation transfer from a $D_2/^4He$ reaction to ionize an alpha particle from a Pd nucleus.

ground state nucleus of the host lattice, as illustrated in Fig. 2. We do not expect a Pd nucleus to have any long-lived excited state in the vicinity of 24 MeV; consequently, this kind of excitation transfer would be an incoherent process.

The initial excitation transfer would create a highly excited compound state [36] which subsequently decays through all available decay channels. Consequently we would expect to see neutron and proton emission as well, and perhaps decays involving heavier products with reduced probabilities. This kind of incoherent excitation transfer process can be described simply within the dynamical model discussed in Appendix B.

Whether this theoretical conjecture concerning excitation transfer is correct or not has at this point not been settled. Unfortunately there has not been a subsequent confirmation of the 21 MeV alpha emission reported in Ref. [35]. On the other hand there have been subsequent reports of energetic alphas (see e.g. [37–41]) as well as energetic neutrons (see Refs. [42,43]). The energetic neutron emission in these latter references is discussed in the context of D+T fusion neutrons; however, as was pointed out earlier the flux of energetic neutrons seems inconsistent with a D+T fusion mechanism [44], which motivates us to consider here an excitation transfer mechanism.

9.1. Alpha energies from $D_2/^4He$ excitation transfer

Of interest is whether there might be some way to prove whether excitation transfer is responsible for energetic alpha emission. One possibility might be to test whether the emitted alpha energy for excitation transfer involving different host lattices matches theory. In Fig. 3 we show the reaction energy and ejected alpha energy including recoil as a function of the nuclear mass A. We see that the ejected alpha energy does depend on the host lattice, and that clarification could be obtained if it were possible to establish a relation between the ejected alpha energy and the nuclear mass of the host lattice.

9.2. Neutron energies from $D_2/^4He$ excitation transfer

Making the case above based on the observation of alpha particles suffers from the complication that alphas created inside a cathode lose energy before making it out of the cathode. Neutrons resulting from incoherent excitation transfer would not be expected to

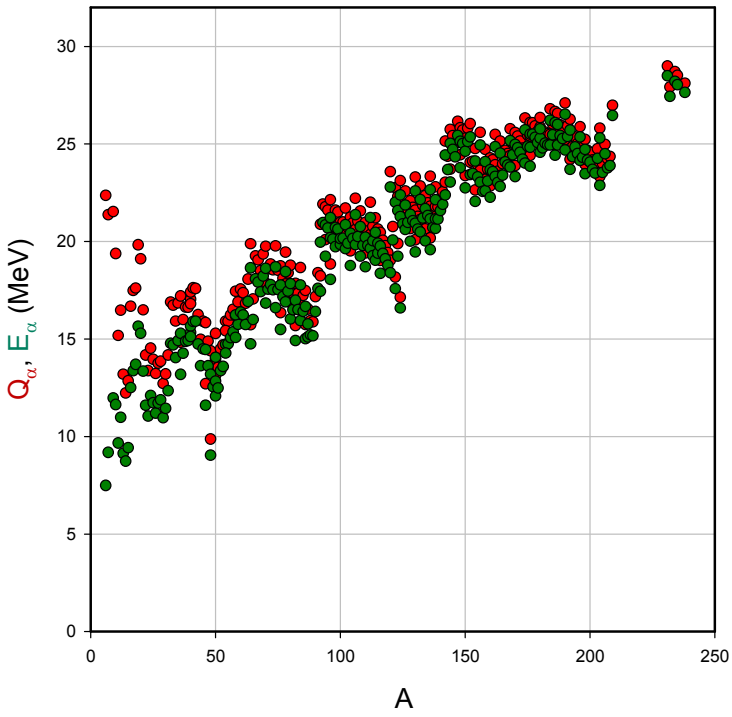

Figure 3. Overall reaction energy (*red*) and ejected alpha energy E_α (*green*) as a function of the initial nuclear mass number A.

lose much energy, and could therefore provide a potentially more faithful diagnostic. The reaction and neutron ejection energy as a function of nuclear mass is shown in Fig. 4.

Plastic track detectors have proven useful for the detection of low-level alpha emission, since they time integrate the signal and are free of electrical noise. These same detectors have been used for low-level neutron emission; however, in this case they suffer from a very low yield, and as yet there does not seem to be a reliable energy calibration in use within our field. Likely a new experiment will be needed with a more standard energy-resolving neutron detector and a source with a higher neutron emission rate.

9.3. Alpha energies from HD/^{3}He excitation transfer

It has long been speculated that HD/^{3}He transitions are responsible for excess heat in the light water experiments; however, at this point there has not been reported any measurements correlating ^{3}He with the energy produced. If HD/^{3}He transitions occur, we might expect to see low-level nuclear emissions resulting from incoherent excitation transfer reactions. In this subsection we consider this possibility.

In Fig. 5 we show the reaction energy and expected alpha energy resulting from excitation transfer as a function of the nuclear mass number A. We see some low energy alphas for nuclei with A on the order of 20 or less, then a gap, and then an increasing alpha energy above mass 60. Not included in this figure are estimates of the associated tunneling factors for the ejected alpha through the Coulomb barrier, which if included would lead to vanishingly low ejection probabilities for all points shown above mass 60.

We draw attention to the low-level alpha emission reported by Storms and Scanlan [45] as perhaps being a result of incoherent excitation transfer from the HD/^{3}He transition to low mass nuclei impurities in the host copper metal (which could account for

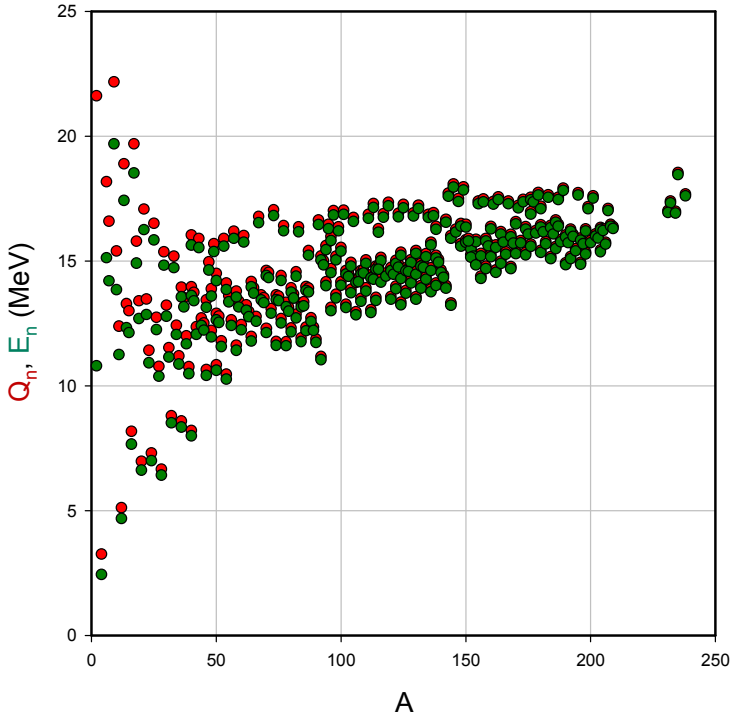

Figure 4. Overall reaction energy (*red*) and ejected neutron energy (*green*) as a function of the initial nuclear mass number A.

alpha emission at a few MeV, but not by itself for the energy shifts reported).

9.4. Neutron energies from HD/^{3}He excitation transfer

Neutron emission resulting from excitation transfer in the case of the HD/^{3}He transition offers the possibility of both gaining evidence for the existence of an excitation transfer effect, and for the possibility that HD/^{3}He transitions can occur. The reaction energy and the ejected neutron energy is shown in Fig. 6 as a function of the nuclear mass number A.

9.5. Proton energies from HD/^{3}He excitation transfer

We conclude this brief discussion by considering proton energies expected in the case of incoherent excitation transfer from HD/^{3}He. The reaction energies and ejected proton energies are shown as a function the nuclear mass number A in Fig. 7. We note that because the HD/^{3}He transition energy (5.49 MeV) is not so large, and generally the proton binding energy tends to be larger, there are only a few nuclei from which one would expect proton ejection. In the figure we see one isotope (^{6}Li) at low mass number and a few at higher mass number, the latter of which have negligible probability of transmission through the Coulomb barrier.

Consequently, our interest in this discussion is focused on the singular case of proton emission for ^{6}Li based on an excitation transfer reaction which we might write as

$$\left[\text{H+D} \rightarrow {}^3\text{He} + 5.49\text{ MeV}\right] + \left[{}^6\text{Li} \rightarrow \text{p} + {}^5\text{He} - 4.43\text{ MeV}\right] + 1.06\text{ MeV}$$

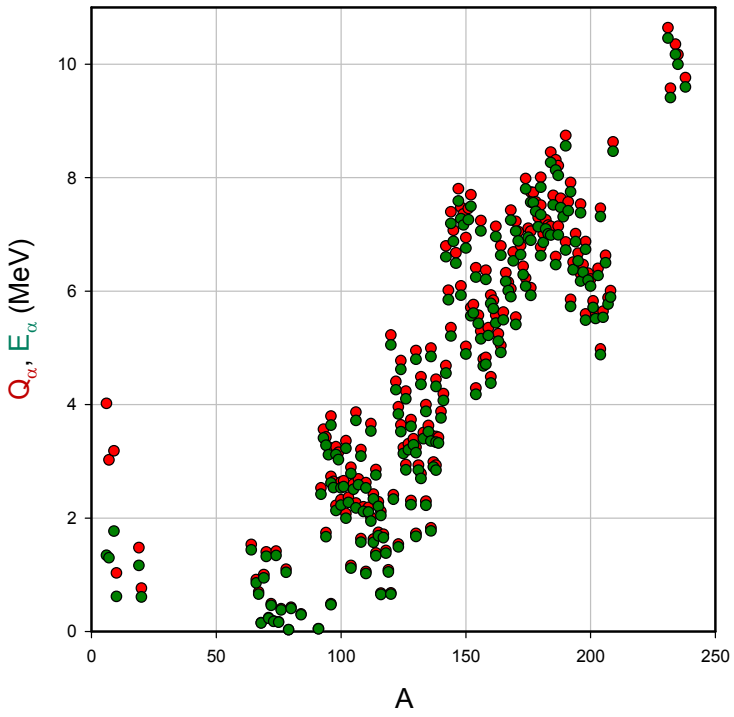

Figure 5. Overall reaction energy (*red*) and ejected alpha energy (*green*) as a function of the initial nuclear mass number A.

leading to an ejected proton energy of 0.88 MeV. We conclude that the observation of proton emission at 0.88 MeV from a lithium sample with H and D present could be argued to support the existence of the corresponding excitation transfer reaction.

9.6. Proton emission in the Lipinski experiment

Many years of experimentation with proton beams on lithium targets, and on glow discharge experiments with hydrogen gas and lithium present, have been documented in Refs. [46,47]. In [47] an experiment is described in which a proton gun is used to irradiate a lithium foil at an energy of a few hundred eV, and that a strong proton signal (identified as "backscattered" protons) is observed at an energy of 0.79 MeV. The data shown in [47] is redrawn in Fig. 8.

Note that the loss of a proton from ^{6}Li would produce a ^{5}He daughter which decays immediately according to

$$^5\text{He} \rightarrow \text{n}(0.59\ \text{MeV}) + {}^4\text{He}(0.15\ \text{MeV}).$$

If these protons are due to excitation transfer, then we might expect to see additional lower energy neutrons and alphas. Note that in the documentation of [47] a brief discussion of neutron detection is given, with the conclusion that no neutrons are detected in connection with the experiment (it is not clear from the documentation whether the neutron detection used would have been sensitive to 0.59 MeV neutrons).

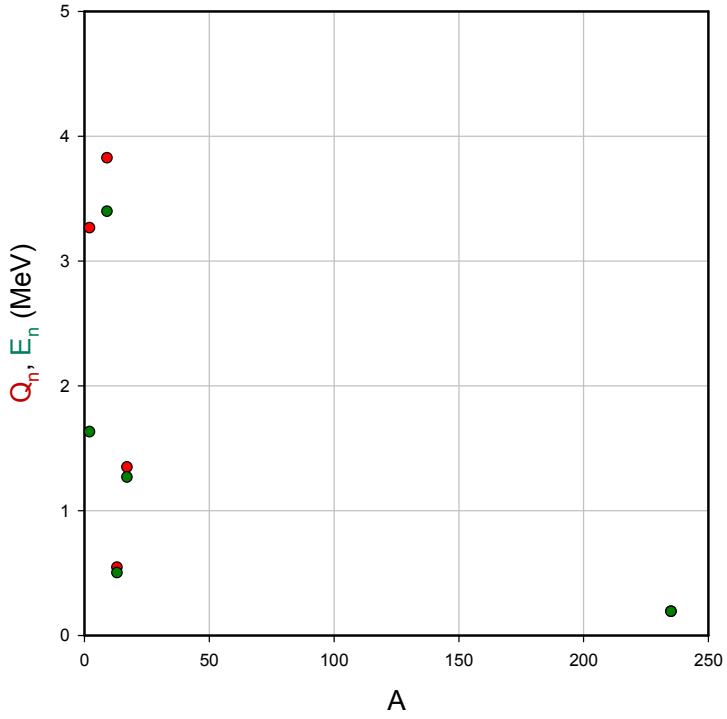

Figure 6. Overall reaction energy (*red*) and ejected neutron energy as a function of the initial nuclear mass number A.

9.7. Alpha emission in the Lipinski experiment

In the same experiment where the proton signal mentioned above was observed, it was reported that energetic alphas were seen near 8.5 MeV. The reported spectrum is redrawn in Fig. 9.

The authors attribute the energetic alpha signal to the H(^{7}Li,α)α reaction (due to a greatly enhanced fusion cross section at the few hundred eV of the incident proton beam). We might write this reaction as

$$\mathrm{H} + {}^7\mathrm{Li} \;\rightarrow\; {}^4\mathrm{He}\ (8.67\ \mathrm{MeV}) + {}^4\mathrm{He}\ (8.67\ \mathrm{MeV})$$

from which it is clear that the alpha energy that results could be consistent with the data of Fig. 9.

We contemplated the possibility of H(^{7}Li,α)α reactions due to the 0.79 MeV protons measured above, but the associated fusion cross section is too low to obtain quantitative agreement.

This motivated us to consider an excitation transfer reaction based on the D_2/^{4}He transition to ^{7}Li, which we might denote according to

$$\left[\mathrm{D{+}D} \;\rightarrow\; {}^4\mathrm{He} + 23.85\ \mathrm{MeV}\right] + \left[{}^7\mathrm{Li} \;\rightarrow\; \mathrm{T} + {}^4\mathrm{He} - 2.47\ \mathrm{MeV}\right] + 21.38\ \mathrm{MeV}.$$

The alpha energy including recoil for this excitation transfer reaction comes out to 9.19 MeV, which is a bit higher than the reported peak energy. Note however that the emission is broad, with an upper end point above 9 MeV. It would be possible to obtain consistency under the assumption that some energy loss in the lithium occurs. The ratio of the energetic alpha emission to proton

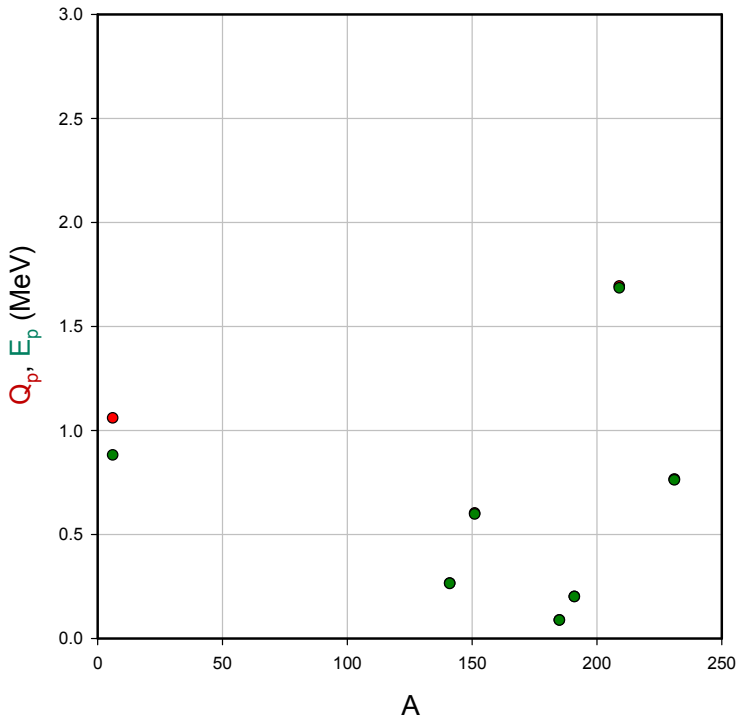

Figure 7. Overall reaction energy (*red*) and ejected proton energy (*green*) as a function of the initial nuclear mass number A.

emission is not too far from the natural isotopic ratio of D to H, as would be expected for this mechanism. According to this excitation transfer reaction proposal we would expect to see energetic tritons at higher energy. There is no mention of such higher energy signals in [47], and the upper energy cut-off of the charged particle detector is too low to see them.

10. Discussion

As we discussed in the Introduction, excitation transfer plays a central role in the phonon-based theory that we have pursued for many years, and is implicated in unexpected non-exponential decay that we have seen in experiments with ^{57}Co in our lab. A major goal of our current research is to work toward the development of theoretical models that can be used to compare directly with experiment, or at least as much as possible. Here we report on recent theoretical results based on the relativistic phonon-nuclear coupling interaction that we identified a few years ago.

We discussed the indirect interaction for resonant excitation transfer in the case of E1 and M1 transitions, from second-order and from fourth-order perturbation theory. This kind of calculation corresponds to the most straightforward application of perturbation theory to the models, based on the relativistic phonon-nuclear interaction. We knew beforehand that destructive interference leads to a small effect for the E1 case which we had analyzed previously. Prior to this study it was unclear whether destructive interference would similarly impact the M1 case – the supposition was that it should, but an erroneous preliminary result suggested that there was some hope that this case might avoid some or most of the destructive interference. From the results of substantial calculations briefly summarized above, we now know that the resonant contribution to the fourth-order interaction relevant to excitation transfer is strongly reduced by destructive interference. The resulting interaction is much too small to connect meaningfully with our

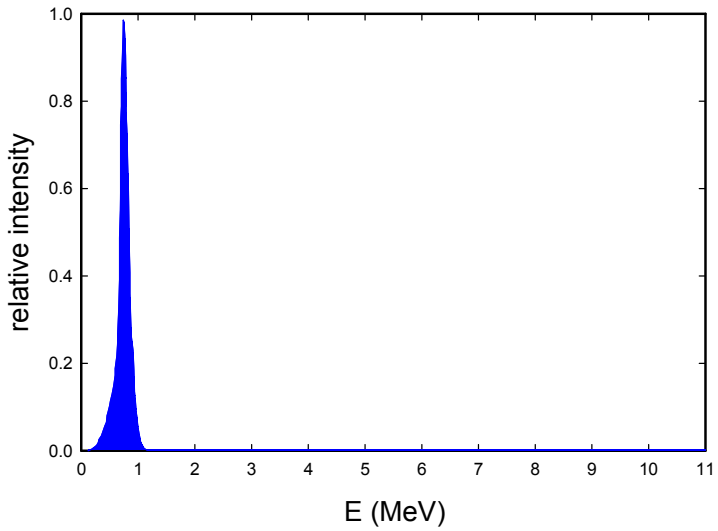

Figure 8. Proton spectrum from experiment #13 from the second Lipinski patent application. The peak location is given as 790 keV, and the peak area is given as 4.2×10^7 counts. The associated count rate is 4.46×10^5 cps.

experimental results.

Destructive interference similarly hinders up-conversion and down-conversion, and we found in 2002 that in models augmented with loss that the destructive interference could be reduced or eliminated. For this problem loss comes in again and again, and the effects are in this way "amplified"; unlike in the case of excitation transfer where loss has a weaker impact. We discussed briefly above the effect of loss on excitation transfer in both E1 and M1 cases, and it is clear that when a relevant THz phonon mode is highly-excited the indirect interaction can be greatly increased. However, it seems unlikely that the indirect interaction that results can be sufficiently large to account for the experimental results. If the experimental results are a result of excitation transfer, then there must be some new additional effect that we have not considered previously.

In the course of writing this paper it became clear that a possible solution to the problem might lie in the variation of the basis state energies that would be expected off of resonance. Developing expressions for the indirect interaction for this kind of model is completely straightforward; however, the quantification of the resulting interactions depends critically on how large the basis state energy shifts are off of resonance. It is possible to make a good argument for the existence of the effect. In the discussion above we outlined a simple argument for it based on the sector decomposition associated with Brillouin-Wigner perturbation theory. In this approach the nucleon-nucleon interaction itself changes off of resonance. To compute the needed energy shifts, one needs to specify the off-resonant extension of the nucleon-nucleon interaction, and then make use of it for nuclear structure calculations. All in all, a big project which we hope to address in the future.

We have evaluated the off-resonant extension of the Breit interaction associated with transverse photon exchange in the Coulomb gauge, which can be used to evaluate the electronic energy shift for atoms and ions off of resonance. The existence of a pole on the k-axis in the result suggests that there might be an associated radiative decay channel; however, for one of the integrals that we are able to evaluate analytically the contribution of the pole turns out to be real, which rules out such a decay channel for this term. More work is needed to clarify whether the pole in the other integral produces an imaginary contribution.

We also outlined recent thoughts as to how the theoretical models connect with our recent excitation transfer experiments. In the experiments we see an angular anisotropy effect associated with the harder gammas, which could be consistent with excitation transfer to nearby nuclei. Within this interpretation it is possible to develop a rough estimate for the indirect coupling matrix

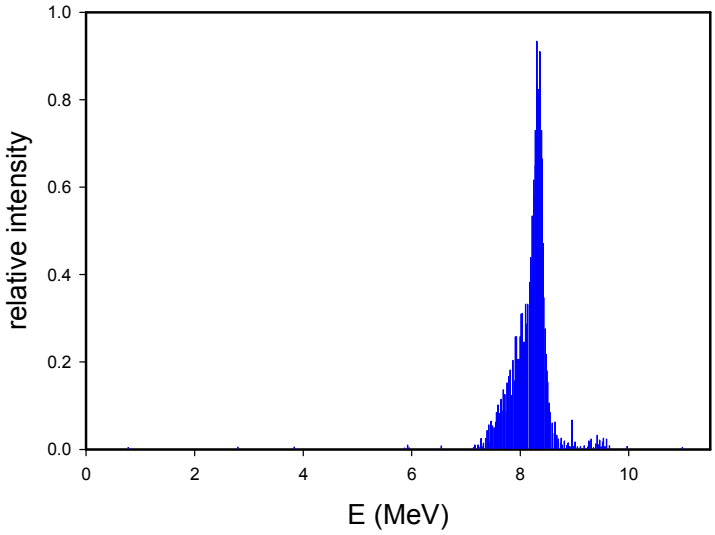

Figure 9. Alphas spectrum from experiment #13 from the second Lipinski patent application. The peak location is given as 8.5 MeV keV (it is closer to 8.3 MeV from the reconstruction in this figure), and the peak area is given as 1.5×10^4 counts. The associated count rate is given as 157 cps.

element. We also see what appears to be a delocalization effect, which may be consistent with the delocalized excitation transfer we see in the models. However, in both cases we are going to need estimates for the off-resonant basis energy shifts to have any hope of quantitative agreement between theory and experiment. Note that what phonon modes are excited, and by how much, is not available in current experiments.

We would very much like to extend the experiments to excitation transfer in E1 transitions. Radioactive sources appear to be available for some higher energy E1 transitions. But what we might learn much more from are excitation transfer experiments with the 6.237 keV transition in ^{181}Ta, for which the relevant radioactive source ^{181}W is currently unavailable from suppliers. This has motivated us to consider new experiments in which excitation transfer might be observed through a modification of the relative Bragg peak intensities in experiments with narrow band synchrotron radiation. Given the large expense associated with synchrotron experiments, such experiments may not be possible any time soon; nevertheless, it seems worthwhile to contemplate such experiments at this time. Note that if such experiments are pursued, it would make sense to demonstrate excitation transfer on the 14.4 keV transition in ^{57}Fe first, since this transition is easier to work with and better studied.

A brief discussion of incoherent excitation transfer reactions based on D_2/^{4}He transitions and HD/^{3}He transitions was given. The idea is that some of the low-level nuclear emissions observed in experiments with PdD may be a result of excitation transfer. Even though the theoretical proposal was put forth in 2000, eighteen years later there has been no confirmation or rejection of this conjecture. One way to sort this out might be to seek a correlation between the emitted particle energy and the masses of the host lattice nuclei. Although we have been thinking about similar emissions driven by the HD/^{3}He transition, it was only recently that we understood that the low-level few MeV alpha emission reported by Storms and Scanlan might be a result of incoherent excitation transfer from the HD/^{3}He transition.

The interesting observations reported by Lipinski and Lipinski have attracted the attention of X. Z. Li in recent years [48]. During the past year it has become clear that incoherent excitation transfer reactions might be involved in the case of the 0.79 MeV proton signal and 8.5 MeV alpha signal reported.

Appendix A. Indirect Interaction for Three Modes

We would generally expect a three-mode interaction to be associated with phonon scattering, rather than with resonant excitation transfer. However, there are conditions under which the three-mode interaction can mediate resonant excitation transfer; for example, when there are three distinct very highly excited modes with surrounding modes unexcited.

As discussed in the text we focused on a particular example in which a phonon from one mode $(\mathbf{k},\sigma)$ is created by one nucleus and absorbed by the other, where a phonon from another mode $(\mathbf{k}',\sigma')$ is created, and where a phonon from a third mode $(\mathbf{k}'',\sigma'')$ is destroyed. The indirect interaction is resonant if the frequencies of the latter two modes are the same.

As discussed in the main text the contribution to the resonant indirect interaction is

$$\left(\hat{V}(E-\hat{H}_0)^{-1}\hat{V}(E-\hat{H}_0)^{-1}\hat{V}(E-\hat{H}_0)^{-1}\hat{V}\right)_{\rm resonant} \rightarrow T_1' + \cdots + T_8'. \tag{A.1}$$

The different contributions $T_1' \cdots T_8'$ are given by

$$\begin{aligned}
T_1' =& \frac{(Mc^2)^2}{4}\sum_{J_2}\sum_{J_2'}\frac{2}{(E_1-E_0)^2(E_2-E_1)(E_2'-E_1)} \\
&\sum_j\sum_{j'}\sum_{m_0}\sum_{m_1}\sum_{m_2}\sum_{m_0'}\sum_{m_1'}\sum_{m_2'}\left(|J_0m_0\rangle\langle J_1m_1|\right)_j\left(|J_1m_1'\rangle\langle J_0m_0'|\right)_{j'} \\
&\langle J_0m_0|\mathbf{a}_j|J_2m_2\rangle\cdot\left[\frac{1}{N}\sum_{\mathbf{k},\sigma}(\hbar\omega_{\mathbf{k},\sigma})^2\mathbf{u}_{\mathbf{k},\sigma}\mathbf{u}_{\mathbf{k},\sigma}\cos\left(\mathbf{k}\cdot(\mathbf{R}_{j'}^{(0)}-\mathbf{R}_j^{(0)})\right)\right]\cdot\langle J_2'm_2'|\mathbf{a}_{j'}|J_0m_0'\rangle \\
&\langle J_2m_2|\mathbf{a}_j|J_1m_1\rangle\cdot\left[\sum_{\mathbf{k}',\sigma'}\sqrt{\hbar\omega_{\mathbf{k}',\sigma'}}\mathbf{u}_{\mathbf{k}',\sigma'}\sqrt{\hat{n}_{\mathbf{k}',\sigma'}+1}\mathrm{e}^{-i\mathbf{k}'\cdot\mathbf{R}_j^{(0)}}\right] \\
&\langle J_1m_1'|\mathbf{a}_{j'}|J_2'm_2'\rangle\cdot\left[\sum_{\mathbf{k}'',\sigma''}\sqrt{\hbar\omega_{\mathbf{k}'',\sigma''}}\mathbf{u}_{\mathbf{k}'',\sigma''}\sqrt{\hat{n}_{\mathbf{k}'',\sigma''}}\mathbf{e}^{i\mathbf{k}''\cdot\mathbf{R}_{j'}^{(0)}}\right],
\end{aligned} \tag{A.2}$$

$$\begin{aligned}
T_2' =& \frac{(Mc^2)^2}{4}\sum_{J_2}\sum_{J_2'}\frac{2}{(E_1-E_0)^2(E_2-E_1)(E_2'-E_0)} \\
&\sum_j\sum_{j'}\sum_{m_0}\sum_{m_1}\sum_{m_2}\sum_{m_0'}\sum_{m_1'}\sum_{m_2'}\left(|J_0m_0\rangle\langle J_1m_1|\right)_j\left(|J_1m_1'\rangle\langle J_0m_0'|\right)_{j'} \\
&\langle J_0m_0|\mathbf{a}_j|J_2m_2\rangle\cdot\left[\frac{1}{N}\sum_{\mathbf{k},\sigma}(\hbar\omega_{\mathbf{k},\sigma})^2\mathbf{u}_{\mathbf{k},\sigma}\mathbf{u}_{\mathbf{k},\sigma}\cos\left(\mathbf{k}\cdot(\mathbf{R}_{j'}^{(0)}-\mathbf{R}_j^{(0)})\right)\right]\cdot\langle J_1m_1'|\mathbf{a}_{j'}|J_2'm_2'\rangle \\
&\langle J_2m_2|\mathbf{a}_j|J_1m_1\rangle\cdot\left[\sum_{\mathbf{k}',\sigma'}\sqrt{\hbar\omega_{\mathbf{k}',\sigma'}}\mathbf{u}_{\mathbf{k}',\sigma'}\sqrt{\hat{n}_{\mathbf{k}',\sigma'}+1}\mathrm{e}^{-i\mathbf{k}'\cdot\mathbf{R}_j^{(0)}}\right] \\
&\langle J_2'm_2'|\mathbf{a}_{j'}|J_0m_0'\rangle\cdot\left[\sum_{\mathbf{k}'',\sigma''}\sqrt{\hbar\omega_{\mathbf{k}'',\sigma''}}\mathbf{u}_{\mathbf{k}'',\sigma''}\sqrt{\hat{n}_{\mathbf{k}'',\sigma''}}\mathbf{e}^{i\mathbf{k}''\cdot\mathbf{R}_{j'}^{(0)}}\right],
\end{aligned} \tag{A.3}$$

$$T_3' = \frac{(Mc^2)^2}{4} \sum_{J_2} \sum_{J_2'} \frac{2}{(E_1 - E_0)^2 (E_2 - E_1)(E_2' - E_1)}$$

$$\sum_j \sum_{j'} \sum_{m_0} \sum_{m_1} \sum_{m_2} \sum_{m_0'} \sum_{m_1'} \sum_{m_2'} \left(|J_0 m_0\rangle\langle J_1 m_1| \right)_j \left(|J_1 m_1'\rangle\langle J_0 m_0'| \right)_{j'}$$

$$\langle J_2 m_2 | \mathbf{a}_j | J_1 m_1 \rangle \cdot \left[\frac{1}{N} \sum_{\mathbf{k},\sigma} (\hbar\omega_{\mathbf{k},\sigma})^2 \mathbf{u}_{\mathbf{k},\sigma} \mathbf{u}_{\mathbf{k},\sigma} \cos\left(\mathbf{k} \cdot (\mathbf{R}_{j'}^{(0)} - \mathbf{R}_j^{(0)}) \right) \right] \cdot \langle J_2' m_2' | \mathbf{a}_{j'} | J_0 m_0' \rangle$$

$$\langle J_0 m_0 | \mathbf{a}_j | J_2 m_2 \rangle \cdot \left[\sum_{\mathbf{k}',\sigma'} \sqrt{\hbar\omega_{\mathbf{k}',\sigma'}} \mathbf{u}_{\mathbf{k}',\sigma'} \sqrt{\hat{n}_{\mathbf{k}',\sigma'} + 1} \mathrm{e}^{-i\mathbf{k}' \cdot \mathbf{R}_j^{(0)}} \right]$$

$$\langle J_1 m_1' | \mathbf{a}_{j'} | J_2' m_2' \rangle \cdot \left[\sum_{\mathbf{k}'',\sigma''} \sqrt{\hbar\omega_{\mathbf{k}'',\sigma''}} \mathbf{u}_{\mathbf{k}'',\sigma''} \sqrt{\hat{n}_{\mathbf{k}'',\sigma''}} \mathbf{e}^{i\mathbf{k}'' \cdot \mathbf{R}_{j'}^{(0)}} \right], \tag{A.4}$$

$$T_4' = \frac{(Mc^2)^2}{4} \sum_{J_2} \sum_{J_2'} \frac{2}{(E_1 - E_0)^2 (E_2 - E_0)(E_2' - E_0)}$$

$$\sum_j \sum_{j'} \sum_{m_0} \sum_{m_1} \sum_{m_2} \sum_{m_0'} \sum_{m_1'} \sum_{m_2'} \left(|J_0 m_0\rangle\langle J_1 m_1| \right)_j \left(|J_1 m_1'\rangle\langle J_0 m_0'| \right)_{j'}$$

$$\langle J_2 m_2 | \mathbf{a}_j | J_1 m_1 \rangle \cdot \left[\frac{1}{N} \sum_{\mathbf{k},\sigma} (\hbar\omega_{\mathbf{k},\sigma})^2 \mathbf{u}_{\mathbf{k},\sigma} \mathbf{u}_{\mathbf{k},\sigma} \cos\left(\mathbf{k} \cdot (\mathbf{R}_{j'}^{(0)} - \mathbf{R}_j^{(0)}) \right) \right] \cdot \langle J_1 m_1' | \mathbf{a}_{j'} | J_2' m_2' \rangle$$

$$\langle J_0 m_0 | \mathbf{a}_j | J_2 m_2 \rangle \cdot \left[\sum_{\mathbf{k}',\sigma'} \sqrt{\hbar\omega_{\mathbf{k}',\sigma'}} \mathbf{u}_{\mathbf{k}',\sigma'} \sqrt{\hat{n}_{\mathbf{k}',\sigma'} + 1} \mathrm{e}^{-i\mathbf{k}' \cdot \mathbf{R}_j^{(0)}} \right]$$

$$\langle J_2' m_2' | \mathbf{a}_{j'} | J_0 m_0' \rangle \cdot \left[\sum_{\mathbf{k}'',\sigma''} \sqrt{\hbar\omega_{\mathbf{k}'',\sigma''}} \mathbf{u}_{\mathbf{k}'',\sigma''} \sqrt{\hat{n}_{\mathbf{k}'',\sigma''}} \mathbf{e}^{i\mathbf{k}'' \cdot \mathbf{R}_{j'}^{(0)}} \right], \tag{A.5}$$

$$T_5' = \frac{(Mc^2)^2}{4} \sum_{J_2} \sum_{J_2'} \frac{2}{(E_1 - E_0)^2 (E_2 - E_1)(E_2' - E_1)}$$

$$\sum_j \sum_{j'} \sum_{m_0} \sum_{m_1} \sum_{m_2} \sum_{m_0'} \sum_{m_1'} \sum_{m_2'} \left(|J_0 m_0\rangle\langle J_1 m_1| \right)_j \left(|J_1 m_1'\rangle\langle J_0 m_0'| \right)_{j'}$$

$$\langle J_0 m_0 | \mathbf{a}_j | J_2 m_2 \rangle \cdot \left[\frac{1}{N} \sum_{\mathbf{k},\sigma} (\hbar\omega_{\mathbf{k},\sigma})^2 \mathbf{u}_{\mathbf{k},\sigma} \mathbf{u}_{\mathbf{k},\sigma} \cos\left(\mathbf{k} \cdot (\mathbf{R}_{j'}^{(0)} - \mathbf{R}_j^{(0)}) \right) \right] \cdot \langle J_2' m_2' | \mathbf{a}_{j'} | J_0 m_0' \rangle$$

$$\langle J_1 m_1' | \mathbf{a}_{j'} | J_2' m_2' \rangle \cdot \left[\sum_{\mathbf{k}',\sigma'} \sqrt{\hbar\omega_{\mathbf{k}',\sigma'}} \mathbf{u}_{\mathbf{k}',\sigma'} \sqrt{\hat{n}_{\mathbf{k}',\sigma'} + 1} \mathrm{e}^{-i\mathbf{k}' \cdot \mathbf{R}_{j'}^{(0)}} \right]$$

$$\langle J_2 m_2 | \mathbf{a}_j | J_1 m_1 \rangle \cdot \left[\sum_{\mathbf{k}'',\sigma''} \sqrt{\hbar\omega_{\mathbf{k}'',\sigma''}} \mathbf{u}_{\mathbf{k}'',\sigma''} \sqrt{\hat{n}_{\mathbf{k}'',\sigma''}} \mathrm{e}^{i\mathbf{k}'' \cdot \mathbf{R}_j^{(0)}} \right], \tag{A.6}$$

$$T_6' = \frac{(Mc^2)^2}{4} \sum_{J_2} \sum_{J_2'} \frac{2}{(E_1 - E_0)^2 (E_2 - E_1)(E_2' - E_0)}$$

$$\sum_j \sum_{j'} \sum_{m_0} \sum_{m_1} \sum_{m_2} \sum_{m_0'} \sum_{m_1'} \sum_{m_2'} \left(|J_0 m_0\rangle\langle J_1 m_1| \right)_j \left(|J_1 m_1'\rangle\langle J_0 m_0'| \right)_{j'}$$

$$\langle J_0 m_0 | \mathbf{a}_j | J_2 m_2 \rangle \cdot \left[\frac{1}{N} \sum_{\mathbf{k},\sigma} (\hbar\omega_{\mathbf{k},\sigma})^2 \mathbf{u}_{\mathbf{k},\sigma} \mathbf{u}_{\mathbf{k},\sigma} \cos\left(\mathbf{k} \cdot (\mathbf{R}_{j'}^{(0)} - \mathbf{R}_j^{(0)}) \right) \right] \cdot \langle J_1 m_1' | \mathbf{a}_{j'} | J_2' m_2' \rangle$$

$$\langle J_2' m_2' | \mathbf{a}_{j'} | J_0 m_0' \rangle \cdot \left[\sum_{\mathbf{k}',\sigma'} \sqrt{\hbar\omega_{\mathbf{k}',\sigma'}} \mathbf{u}_{\mathbf{k}',\sigma'} \sqrt{\hat{n}_{\mathbf{k}',\sigma'} + 1} \mathrm{e}^{-i\mathbf{k}' \cdot \mathbf{R}_{j'}^{(0)}} \right]$$

$$\langle J_2 m_2 | \mathbf{a}_j | J_1 m_1 \rangle \cdot \left[\sum_{\mathbf{k}'',\sigma''} \sqrt{\hbar\omega_{\mathbf{k}'',\sigma''}} \mathbf{u}_{\mathbf{k}'',\sigma''} \sqrt{\hat{n}_{\mathbf{k}'',\sigma''}} \mathrm{e}^{i\mathbf{k}'' \cdot \mathbf{R}_j^{(0)}} \right], \tag{A.7}$$

$$T_7' = \frac{(Mc^2)^2}{4} \sum_{J_2} \sum_{J_2'} \frac{2}{(E_1 - E_0)^2 (E_2 - E_0)(E_2' - E_1)}$$
$$\sum_j \sum_{j'} \sum_{m_0} \sum_{m_1} \sum_{m_2} \sum_{m_0'} \sum_{m_1'} \sum_{m_2'} \left(|J_0 m_0\rangle\langle J_1 m_1| \right)_j \left(|J_1 m_1'\rangle\langle J_0 m_0'| \right)_{j'}$$
$$\langle J_2 m_2 | \mathbf{a}_j | J_1 m_1 \rangle \cdot \left[\frac{1}{N} \sum_{\mathbf{k},\sigma} (\hbar\omega_{\mathbf{k},\sigma})^2 \mathbf{u}_{\mathbf{k},\sigma} \mathbf{u}_{\mathbf{k},\sigma} \cos\left(\mathbf{k} \cdot (\mathbf{R}_{j'}^{(0)} - \mathbf{R}_j^{(0)}) \right) \right] \cdot \langle J_2' m_2' | \mathbf{a}_{j'} | J_0 m_0' \rangle$$
$$\langle J_1 m_1' | \mathbf{a}_{j'} | J_2' m_2' \rangle \cdot \left[\sum_{\mathbf{k}',\sigma'} \sqrt{\hbar\omega_{\mathbf{k}',\sigma'}} \mathbf{u}_{\mathbf{k}',\sigma'} \sqrt{\hat{n}_{\mathbf{k}',\sigma'} + 1} e^{-i\mathbf{k}' \cdot \mathbf{R}_{j'}^{(0)}} \right]$$
$$\langle J_0 m_0 | \mathbf{a}_j | J_2 m_2 \rangle \cdot \left[\sum_{\mathbf{k}'',\sigma''} \sqrt{\hbar\omega_{\mathbf{k}'',\sigma''}} \mathbf{u}_{\mathbf{k}'',\sigma''} \sqrt{\hat{n}_{\mathbf{k}'',\sigma''}} e^{i\mathbf{k}'' \cdot \mathbf{R}_j^{(0)}} \right], \tag{A.8}$$

$$T_8' = \frac{(Mc^2)^2}{4} \sum_{J_2} \sum_{J_2'} \frac{2}{(E_1 - E_0)^2 (E_2 - E_0)(E_2' - E_0)}$$
$$\sum_j \sum_{j'} \sum_{m_0} \sum_{m_1} \sum_{m_2} \sum_{m_0'} \sum_{m_1'} \sum_{m_2'} \left(|J_0 m_0\rangle\langle J_1 m_1| \right)_j \left(|J_1 m_1'\rangle\langle J_0 m_0'| \right)_{j'}$$
$$\langle J_2 m_2 | \mathbf{a}_j | J_1 m_1 \rangle \cdot \left[\frac{1}{N} \sum_{\mathbf{k},\sigma} (\hbar\omega_{\mathbf{k},\sigma})^2 \mathbf{u}_{\mathbf{k},\sigma} \mathbf{u}_{\mathbf{k},\sigma} \cos\left(\mathbf{k} \cdot (\mathbf{R}_{j'}^{(0)} - \mathbf{R}_j^{(0)}) \right) \right] \cdot \langle J_1 m_1' | \mathbf{a}_{j'} | J_2' m_2' \rangle$$
$$\langle J_2' m_2' | \mathbf{a}_{j'} | J_0 m_0' \rangle \cdot \left[\sum_{\mathbf{k}',\sigma'} \sqrt{\hbar\omega_{\mathbf{k}',\sigma'}} \mathbf{u}_{\mathbf{k}',\sigma'} \sqrt{\hat{n}_{\mathbf{k}',\sigma'} + 1} e^{-i\mathbf{k}' \cdot \mathbf{R}_{j'}^{(0)}} \right]$$
$$\langle J_0 m_0 | \mathbf{a}_j | J_2 m_2 \rangle \cdot \left[\sum_{\mathbf{k}'',\sigma''} \sqrt{\hbar\omega_{\mathbf{k}'',\sigma''}} \mathbf{u}_{\mathbf{k}'',\sigma''} \sqrt{\hat{n}_{\mathbf{k}'',\sigma''}} e^{i\mathbf{k}'' \cdot \mathbf{R}_j^{(0)}} \right]. \tag{A.9}$$

Destructive interference has greatly reduced the total indirect interaction in this case from the strength of contributions from individual pathways.

Appendix B. Dynamical Model for Resonant Excitation Transfer

We are interested in the dynamics associated with excitation transfer between two sites in the presence of an oscillatory driving term. The basic idea is to make use of two two-level systems which are coupled together via excitation transfer, and then develop evolution equations using Ehrenfest's theorem.

Appendix B.1. Idealized model

We can describe a simplified version of the model based on a Hamiltonian of the form

$$\hat{H} = -\frac{1}{2}\Delta E \begin{bmatrix} 1 & 0 & 0 & 0 \\ 0 & -1 & 0 & 0 \\ 0 & 0 & 1 & 0 \\ 0 & 0 & 0 & -1 \end{bmatrix} + V_0 \mathrm{e}^{-i\omega t} \begin{bmatrix} 0 & \mathrm{e}^{i\mathbf{k}\cdot\mathbf{r}_1} & 0 & 0 \\ \mathrm{e}^{i\mathbf{k}\cdot\mathbf{r}_1} & 0 & 0 & 0 \\ 0 & 0 & 0 & \mathrm{e}^{i\mathbf{k}\cdot\mathbf{r}_2} \\ 0 & 0 & \mathrm{e}^{i\mathbf{k}\cdot\mathbf{r}_2} & 0 \end{bmatrix} + U_0 \begin{bmatrix} 0 & 0 & 1 & 0 \\ 0 & 0 & 0 & 1 \\ 1 & 0 & 0 & 0 \\ 0 & 1 & 0 & 0 \end{bmatrix}. \tag{B.1}$$

The first term on the right-hand side describes a pair of two-level systems both with a transition energy ΔE; the second term describes an oscillatory driving term at frequency ω with position phase factors such as would be produced by X-rays from a synchrotron source; and the third term describes coupling via resonant excitation transfer.

Appendix B.2. Evolution equations

We can make use of Ehrenfest's theorem to develop evolution equations according to

$$\frac{\mathrm{d}}{\mathrm{d}t}\langle\hat{Q}\rangle = \left\langle \frac{\partial \hat{Q}}{\partial t} \right\rangle + \frac{1}{i\hbar}\langle[\hat{Q}, \hat{H}]\rangle. \tag{B.2}$$

Following the approach used for the dynamics of the two-level system we can define equivalent two-level system operators within the context of this four level system according to

$$\hat{\sigma}_x^{(1)} = \begin{bmatrix} 0 & 1 & 0 & 0 \\ 1 & 0 & 0 & 0 \\ 0 & 0 & 0 & 0 \\ 0 & 0 & 0 & 0 \end{bmatrix}, \quad \hat{\sigma}_y^{(1)} = \begin{bmatrix} 0 & -i & 0 & 0 \\ i & 0 & 0 & 0 \\ 0 & 0 & 0 & 0 \\ 0 & 0 & 0 & 0 \end{bmatrix}, \quad \hat{\sigma}_z^{(1)} = \begin{bmatrix} 1 & 0 & 0 & 0 \\ 0 & -1 & 0 & 0 \\ 0 & 0 & 0 & 0 \\ 0 & 0 & 0 & 0 \end{bmatrix},$$

$$\hat{\sigma}_x^{(2)} = \begin{bmatrix} 0 & 0 & 0 & 0 \\ 0 & 0 & 0 & 0 \\ 0 & 0 & 0 & 1 \\ 0 & 0 & 1 & 0 \end{bmatrix}, \quad \hat{\sigma}_y^{(1)} = \begin{bmatrix} 0 & 0 & 0 & 0 \\ 0 & 0 & 0 & 0 \\ 0 & 0 & 0 & -i \\ 0 & 0 & i & 0 \end{bmatrix}, \quad \hat{\sigma}_z^{(2)} = \begin{bmatrix} 0 & 0 & 0 & 0 \\ 0 & 0 & 0 & 0 \\ 0 & 0 & 1 & 0 \\ 0 & 0 & 0 & -1 \end{bmatrix}. \tag{B.3}$$

Evolution equations for the expectation values of these operators are

$$\frac{\mathrm{d}}{\mathrm{d}t}\langle\hat{\sigma}_x^{(1)}\rangle = \frac{\Delta E}{\hbar}\langle\hat{\sigma}_y^{(1)}\rangle + \frac{U_0}{\hbar}\langle\hat{A}\rangle, \tag{B.4}$$

$$\frac{\mathrm{d}}{\mathrm{d}t}\langle\hat{\sigma}_x^{(2)}\rangle = \frac{\Delta E}{\hbar}\langle\hat{\sigma}_y^{(2)}\rangle - \frac{U_0}{\hbar}\langle\hat{A}\rangle, \tag{B.5}$$

$$\frac{\mathrm{d}}{\mathrm{d}t}\langle\hat{\sigma}_y^{(1)}\rangle = -\frac{\Delta E}{\hbar}\langle\hat{\sigma}_x^{(1)}\rangle - \frac{2V_0}{\hbar}\mathrm{e}^{i\mathbf{k}\cdot\mathbf{r}_1}\mathrm{e}^{-i\omega t}\langle\hat{\sigma}_z^{(1)}\rangle + \frac{U_0}{\hbar}\langle\hat{B}\rangle, \tag{B.6}$$

$$\frac{\mathrm{d}}{\mathrm{d}t}\langle\hat{\sigma}_y^{(2)}\rangle = -\frac{\Delta E}{\hbar}\langle\hat{\sigma}_x^{(2)}\rangle - \frac{2V_0}{\hbar}\mathrm{e}^{i\mathbf{k}\cdot\mathbf{r}_2}\mathrm{e}^{-i\omega t}\langle\hat{\sigma}_z^{(2)}\rangle - \frac{U_0}{\hbar}\langle\hat{B}\rangle, \tag{B.7}$$

$$\frac{\mathrm{d}}{\mathrm{d}t}\langle\hat{\sigma}_z^{(1)}\rangle = -\frac{2V_0}{\hbar}\mathrm{e}^{i\mathbf{k}\cdot\mathbf{r}_1}\mathrm{e}^{-i\omega t}\langle\hat{\sigma}_y^{(1)}\rangle - \frac{U_0}{\hbar}\langle\hat{D}\rangle, \tag{B.8}$$

$$\frac{\mathrm{d}}{\mathrm{d}t}\langle\hat{\sigma}_z^{(2)}\rangle = -\frac{2V_0}{\hbar}\mathrm{e}^{i\mathbf{k}\cdot\mathbf{r}_2}\mathrm{e}^{-i\omega t}\langle\hat{\sigma}_y^{(2)}\rangle + \frac{U_0}{\hbar}\langle\hat{D}\rangle, \tag{B.9}$$

where we define new operators according to

$$\hat{A} = \begin{bmatrix} 0 & 0 & 0 & -i \\ 0 & 0 & -i & 0 \\ 0 & i & 0 & 0 \\ i & 0 & 0 & 0 \end{bmatrix}, \quad \hat{B} = \begin{bmatrix} 0 & 0 & 0 & -1 \\ 0 & 0 & 1 & 0 \\ 0 & 1 & 0 & 0 \\ -1 & 0 & 0 & 0 \end{bmatrix},$$

$$\hat{C} = \begin{bmatrix} 0&0&1&0 \\ 0&0&0&1 \\ 1&0&0&0 \\ 0&1&0&0 \end{bmatrix}, \quad \hat{D} = \begin{bmatrix} 0&0&i&0 \\ 0&0&0&-i \\ -i&0&0&0 \\ 0&i&0&0 \end{bmatrix}. \tag{B.10}$$

Evolution equations associated with these operators are

$$\frac{\mathrm{d}}{\mathrm{d}t}\langle\hat{A}\rangle = \frac{\Delta E}{\hbar}\langle\hat{B}\rangle + \frac{2V_0}{\hbar}\mathrm{e}^{i\mathbf{k}\cdot\mathbf{r}_1}\mathrm{e}^{-i\omega t}\langle\hat{C}\rangle - \frac{2V_0}{\hbar}\,\mathrm{e}^{i\mathbf{k}\cdot\mathbf{r}_2}\mathrm{e}^{-i\omega t}\langle\hat{C}\rangle - \frac{2U_0}{\hbar}\langle\hat{\sigma}_x^{(1)} - \hat{\sigma}_x^{(2)}\rangle, \tag{B.11}$$

$$\frac{\mathrm{d}}{\mathrm{d}t}\langle\hat{B}\rangle = -\frac{\Delta E}{\hbar}\langle\hat{A}\rangle + \frac{2V_0}{\hbar}\mathrm{e}^{i\mathbf{k}\cdot\mathbf{r}_1}\mathrm{e}^{-i\omega t}\langle\hat{D}\rangle + \frac{2V_0}{\hbar}\mathrm{e}^{i\mathbf{k}\cdot\mathbf{r}_2}\mathrm{e}^{-i\omega t}\langle\hat{D}\rangle - \frac{2U_0}{\hbar}\langle\hat{\sigma}_y^{(1)} - \hat{\sigma}_y^{(2)}\rangle, \tag{B.12}$$

$$\frac{\mathrm{d}}{\mathrm{d}t}\langle\hat{C}\rangle = -\frac{2V_0}{\hbar}\mathrm{e}^{i\mathbf{k}\cdot\mathbf{r}_1}\mathrm{e}^{-i\omega t}\langle\hat{A}\rangle + \frac{2V_0}{\hbar}\mathrm{e}^{i\mathbf{k}\cdot\mathbf{r}_2}\mathrm{e}^{-i\omega t}\langle\hat{A}\rangle, \tag{B.13}$$

$$\frac{\mathrm{d}}{\mathrm{d}t}\langle\hat{D}\rangle = -\frac{2V_0}{\hbar}\mathrm{e}^{i\mathbf{k}\cdot\mathbf{r}_1}\mathrm{e}^{-i\omega t}\langle\hat{B}\rangle - \frac{2V_0}{\hbar}\mathrm{e}^{i\mathbf{k}\cdot\mathbf{r}_2}\mathrm{e}^{-i\omega t}\langle\hat{B}\rangle + \frac{2U_0}{\hbar}\langle\hat{\sigma}_z^{(1)} - \hat{\sigma}_z^{(2)}\rangle. \tag{B.14}$$

Due to the relative simplicity of this model we are able to describe the dynamics of the associated expectation values with only 10 first-order equations.

Appendix B.3. Empirical loss

For the two-level system model the associated Bloch equations can be augmented with an empirical loss model. Given the similarity with the model here, we propose the generalization

$$\left(\frac{\mathrm{d}}{\mathrm{d}t} + \frac{1}{T_2}\right)\langle\hat{\sigma}_x^{(1)}\rangle = \frac{\Delta E}{\hbar}\langle\hat{\sigma}_y^{(1)}\rangle + \frac{U_0}{\hbar}\langle\hat{A}\rangle \tag{B.15}$$

$$\left(\frac{\mathrm{d}}{\mathrm{d}t} + \frac{1}{T_2}\right)\langle\hat{\sigma}_x^{(2)}\rangle = \frac{\Delta E}{\hbar}\langle\hat{\sigma}_y^{(2)}\rangle - \frac{U_0}{\hbar}\langle\hat{A}\rangle \tag{B.16}$$

$$\left(\frac{\mathrm{d}}{\mathrm{d}t} + \frac{1}{T_2}\right)\langle\hat{\sigma}_y^{(1)}\rangle = -\frac{\Delta E}{\hbar}\langle\hat{\sigma}_x^{(1)}\rangle - \frac{2V_0}{\hbar}\mathrm{e}^{i\mathbf{k}\cdot\mathbf{r}_1}\mathrm{e}^{-i\omega t}\langle\hat{\sigma}_z^{(1)}\rangle + \frac{U_0}{\hbar}\langle\hat{B}\rangle, \tag{B.17}$$

$$\left(\frac{\mathrm{d}}{\mathrm{d}t} + \frac{1}{T_2}\right)\langle\hat{\sigma}_y^{(2)}\rangle = -\frac{\Delta E}{\hbar}\langle\hat{\sigma}_x^{(2)}\rangle - \frac{2V_0}{\hbar}\mathrm{e}^{i\mathbf{k}\cdot\mathbf{r}_2}\mathrm{e}^{-i\omega t}\langle\hat{\sigma}_z^{(2)}\rangle - \frac{U_0}{\hbar}\langle\hat{B}\rangle, \tag{B.18}$$

$$\frac{\mathrm{d}}{\mathrm{d}t}\langle\hat{\sigma}_z^{(1)}\rangle + \frac{\langle\hat{\sigma}_z^{(1)}\rangle - \sigma_{z0}^{(1)}}{T_1} = -\frac{2V_0}{\hbar}\mathrm{e}^{i\mathbf{k}\cdot\mathbf{r}_1}\mathrm{e}^{-i\omega t}\langle\hat{\sigma}_y^{(1)}\rangle - \frac{U_0}{\hbar}\langle\hat{D}\rangle, \tag{B.19}$$

$$\frac{\mathrm{d}}{\mathrm{d}t}\langle\hat{\sigma}_z^{(2)}\rangle + \frac{\langle\hat{\sigma}_z^{(2)}\rangle - \sigma_{z0}^{(2)}}{T_1} = -\frac{2V_0}{\hbar}\mathrm{e}^{i\mathbf{k}\cdot\mathbf{r}_2}\mathrm{e}^{-i\omega t}\langle\hat{\sigma}_y^{(2)}\rangle + \frac{U_0}{\hbar}\langle\hat{D}\rangle, \tag{B.20}$$

$$\left(\frac{\mathrm{d}}{\mathrm{d}t} + \frac{1}{T_{X2}}\right)\langle\hat{A}\rangle = \frac{\Delta E}{\hbar}\langle\hat{B}\rangle + \frac{2V_0}{\hbar}\mathrm{e}^{i\mathbf{k}\cdot\mathbf{r}_1}\mathrm{e}^{-i\omega t}\langle\hat{C}\rangle - \frac{2V_0}{\hbar}\mathrm{e}^{i\mathbf{k}\cdot\mathbf{r}_2}\mathrm{e}^{-i\omega t}\langle\hat{C}\rangle - \frac{2U_0}{\hbar}\langle\hat{\sigma}_x^{(1)} - \hat{\sigma}_x^{(2)}\rangle, \tag{B.21}$$

$$\left(\frac{\mathrm{d}}{\mathrm{d}t} + \frac{1}{T_{X2}}\right)\langle\hat{B}\rangle = -\frac{\Delta E}{\hbar}\langle\hat{A}\rangle + \frac{2V_0}{\hbar}e^{i\mathbf{k}\cdot\mathbf{r}_1}\mathrm{e}^{-i\omega t}\langle\hat{D}\rangle + \frac{2V_0}{\hbar}\mathrm{e}^{i\mathbf{k}\cdot\mathbf{r}_2}\mathrm{e}^{-i\omega t}\langle\hat{D}\rangle - \frac{2U_0}{\hbar}\langle\hat{\sigma}_y^{(1)} - \hat{\sigma}_y^{(2)}\rangle, \tag{B.22}$$

$$\left(\frac{\mathrm{d}}{\mathrm{d}t} + \frac{1}{T_{X1}}\right)\langle\hat{C}\rangle = -\frac{2V_0}{\hbar}\mathrm{e}^{i\mathbf{k}\cdot\mathbf{r}_1}\mathrm{e}^{-i\omega t}\langle\hat{A}\rangle + \frac{2V_0}{\hbar}\mathrm{e}^{i\mathbf{k}\cdot\mathbf{r}_2}\mathrm{e}^{-i\omega t}\langle\hat{A}\rangle, \tag{B.23}$$

$$\left(\frac{\mathrm{d}}{\mathrm{d}t}+\frac{1}{T_{X1}}\right)\langle\hat{D}\rangle=-\frac{2V_0}{\hbar}\mathrm{e}^{i\mathbf{k}\cdot\mathbf{r}_1}\mathrm{e}^{-i\omega t}\langle\hat{B}\rangle-\frac{2V_0}{\hbar}\mathrm{e}^{i\mathbf{k}\cdot\mathbf{r}_2}\mathrm{e}^{-i\omega t}\langle\hat{B}\rangle+\frac{2U_0}{\hbar}\langle\hat{\sigma}_z^{(1)}-\hat{\sigma}_z^{(2)}\rangle \tag{B.24}$$

with T_{X1} and T_{X2} providing direct extensions of T_1 and T_2 for relaxation times associated with excitation transfer related population and polarization operators.

Appendix B.4. Simple solution with no driving term

Suppose that we have two idealized equivalent nuclei in proximity with resonant excitation transfer and no X-ray driving term. If we assume that the T_{X1} relaxation time associated with excitation transfer is the same as the two-level relaxation time T_1, then we can write

$$\left(\frac{\mathrm{d}}{\mathrm{d}t}+\frac{1}{T_1}\right)\langle\hat{\sigma}_z^{(1)}-\hat{\sigma}_z^{(2)}\rangle=-\frac{2U_0}{\hbar}\langle\hat{D}\rangle, \tag{B.25}$$

$$\left(\frac{\mathrm{d}}{\mathrm{d}t}+\frac{1}{T_1}\right)\langle\hat{D}\rangle=\frac{2U_0}{\hbar}\langle\hat{\sigma}_z^{(1)}-\hat{\sigma}_z^{(2)}\rangle. \tag{B.26}$$

A relevant solution to these equations is

$$\langle\hat{\sigma}_z^{(1)}-\hat{\sigma}_z^{(2)}\rangle=2\mathrm{e}^{-t/T_1}\cos\left(\frac{2U_0}{\hbar}t\right). \tag{B.27}$$

In this model the occupation probability oscillates back and forth, decaying with the expected decay constant for an excited state.

Appendix B.5. Excitation transfer to an unstable final state

Suppose that we start with a nuclear system in a stable excited state in proximity to a nucleus in a stable ground state, where excitation transfer couples to a final state where the upper state of the newly promoted excited nucleus is very unstable. In this case we can develop a simplified description according to

$$\frac{\mathrm{d}}{\mathrm{d}t}\langle\hat{\sigma}_z^{(1)}\rangle=-\frac{U_0}{\hbar}\langle\hat{D}\rangle, \tag{B.28}$$

$$\frac{\mathrm{d}}{\mathrm{d}t}\langle\hat{\sigma}_z^{(2)}\rangle+\frac{\langle\hat{\sigma}_z^{(2)}\rangle-\sigma_{z0}^{(2)}}{T_1}=\frac{U_0}{\hbar}\langle\hat{D}\rangle, \tag{B.29}$$

$$\left(\frac{\mathrm{d}}{\mathrm{d}t}+\frac{1}{T_1}\right)\langle\hat{D}\rangle=\frac{2U_0}{\hbar}\langle\hat{\sigma}_z^{(1)}-\hat{\sigma}_z^{(2)}\rangle, \tag{B.30}$$

where we have assumed that the destruction of the excitation transfer term is dominated by the decay rate of the unstable excited state. We can solve approximately for $\langle\hat{D}\rangle$ to get

$$\langle\hat{D}\rangle=\frac{2U_0}{\hbar}T_1\langle\hat{\sigma}_z^{(1)}-\hat{\sigma}_z^{(2)}\rangle. \tag{B.31}$$

We can make use of this to develop an estimate for the loss of the initial excitation

$$\frac{\mathrm{d}}{\mathrm{d}t}\langle\hat{\sigma}_z^{(1)}\rangle=-2\left(\frac{U_0}{\hbar}\right)^2T_1\langle\hat{\sigma}_z^{(1)}-\hat{\sigma}_z^{(2)}\rangle. \tag{B.32}$$

Appendix C. Impact on Internal Conversion

A reviewer has noted that we do not appear to consider the impact of internal conversion on the model, and on the excitation transfer process, and encouraged us to provide some discussion.

We note that an excited nuclear state can decay radiatively, and generally can also decay through internal conversion wherein the nucleus is de-excited with the excitation energy split between the electron removal energy and kinetic energy. In our experiments we can see gammas at 14.4 keV associated with the radiative decay of the 14.4 keV excited state of ^{57}Fe, and also the Fe K_α results from K-shell holes created via the absorption of a K-shell electron by the ^{57}Co nucleus during beta decay as well as from the internal conversion of the 14.4 keV state. Internal conversion of the highly-excited 136.5 keV state is much weaker, resulting in only a minor contribution to the creation of K-shell holes [49].

In general, a high internal conversion coefficient means that the efficiency of gamma emission is reduced, which generally makes it technically more difficult to carry out an experiment. For example, there are no Mossbauer experiments with the 1.565 keV transition in ^{201}Hg which has a very high internal conversion coefficient.

We would not expect phonon exchange and excitation transfer to have much effect on the internal conversion rate for states that are on resonance, primarily since it is so difficult to have much of an impact on the structure of an excited nuclear state, on a K-shell electronic orbital, or on the energy available for internal conversion. The reviewer has argued that in the presence of a highly-excited phonon mode that it is possible for the electron orbitals to be modified, resulting in changes to the rate for internal conversion. This may be true for the small contribution to internal conversion from the outer electron orbitals that could be modified due to strong lattice vibrations, and would require electron spectroscopy to see. We have not found papers in the literature discussing theory or experimental results for this.

In the absence of loss mechanisms we would expect resonant excitation transfer to be efficient in transferring excitation from one nucleus to another. However, loss can greatly reduce the efficiency for resonant excitation transfer, as can be seen in the model discussed briefly in Appendix B. For low energy nuclear transitions we would expect the dominant loss mechanism to be internal conversion, so the internal conversion rate in general will limit how much excitation is transferred. In this case the T_1 and T_{X1} parameters in the model will be dominated by internal conversion.

In a recent free-electron laser experiment the acceleration of the radiative decay of excited nuclei has been observed due to Dicke superradiance [50]. In such an experiment the internal conversion coefficient would be changed since the radiative decay rate is accelerated.

There appear discussions in the literature of possible modifications of the rate of internal conversion due to resonances [51] and an electron bridge [52].

In the main text there is a discussion of the possible acceleration of the rate for excitation transfer due to loss effects, as long as the loss for the different basis states is changed. For the nuclear part of the problem this involves internal conversion for low-energy nuclear transitions.

We have discussed in the text a modification of the incremental ratio of the 14.4 keV intensity relative to the Fe K_α intensity in our excitation transfer experiments. As discussed above we are considering an interpretation of this involving new decay channels opening for off-resonant basis states.

References

[1] M. Fleischmann, S. Pons and M. Hawkins, *J. Electroanal Chem.* **201** (1989) 301; errata, **263** (1990) 187.
[2] M. Fleischmann, S. Pons, M.W. Anderson, L.J. Li and M. Hawkins, *J. Electroanal. Chem.* **287** (1990) 293.
[3] P.L. Hagelstein, Current status of the theory and modeling effort based on fractionation, *J. Condensed Matter Nucl. Sci.* **19** (2016) 98–109.
[4] P.L. Hagelstein, Quantum Composites: A review and new results for condensed matter nuclear science, *J. Condensed Matter Nucl. Sci.* **20** (2016) 139–225.
[5] P.L. Hagelstein, A unified model for anomalies in metal deuterides, *Proc. ICCF9* (2002) 121–134.
[6] P.L. Hagelstein and I.U. Chaudhary, Energy exchange in the lossy spin–boson model, *J. Cond. Mat. Nucl. Sci.* **5** (2011) 52.
[7] P.L. Hagelstein and I.U. Chaudhary, Second-order formulation and scaling in the lossy spin–boson model, *J. Cond. Mat. Nucl. Sci.* **5** (2011) 87.

[8] P.L. Hagelstein and I.U. Chaudhary, Local approximation for the lossy spin–boson model, *J. Cond. Mat. Nucl. Sci.* **5** (2011) 102.
[9] P.L. Hagelstein and I.U. Chaudhary, Coherent energy exchange in the strong coupling limit of the lossy spin–boson model, *J. Cond. Mat. Nucl. Sci.* **5** (2011) 116.
[10] F. Metzler, P.L. Hagelstein and S. Lu, Observation of non-exponential decay in X-ray and γ emission lines from Co-57, *J. Condensed Matter Nucl. Sci.*, to appear.
[11] Th. Förster, Zwischenmolekulare Energiewanderung und Fluoreszenz, *Annalen der Phyzik* **6** (1948) 55–75.
[12] D.L. Andrews and A.A. Demidov, *Resonant Excitation Transfer*, Wiley, New York, 1999.
[13] S. Lu, Exploring possible coupling between phonons and internal nuclear states, *MIT PhD Thesis*, Cambridge, MA, USA, 2018.
[14] P.L. Hagelstein and I.U. Chaudhary, Coupling between the center of mass and relative degrees of freedom in a relativistic quantum composite and applications, *J. Condensed Matter Nucl. Sci.* **19** (2016) 98–109.
[15] P.L. Hagelstein and I.U. Chaudhary, Including nuclear degrees of freedom in a lattice Hamiltonian, *J. Condensed Matter Nucl. Sci.* **7** (2012) 35–50.
[16] P.L. Hagelstein and I.U. Chaudhary, Phonon–nuclear coupling for anomalies in Condensed Matter Nuclear Science, *J. Condensed Matter Nucl. Sci.* **12** (2013) 105–142.
[17] M. Mohseni, P. Rebentrost, S. Lloyd and A. Aspuru-Guzik, Environment-assisted quantum walks in photosynthetic energy transfer, *J. Chem. Phys.* **129** (2008) 174106.
[18] M.B. Plenio and S.F. Huelga, Dephasing-assisted transport: quantum networks and biomolecules, *New J. Phys.* **10** (2008) 113019.
[19] R. Laughlin and B.L. Scott, Off-energy-shell t-matrix elements for local potentials containing hard cores, *Phys. Rev.* **171** (1968) 1196–1201.
[20] M.K. Srivastava and D.W.L. Sprung, Off-shell behavior of the nucleon-nucleon interaction, *Adv. Nucl. Phys.* **8** (1975) 121–218.
[21] O. Zohni, Investigation of off-shell effects in triton binding-energy calculations with nonlocal-core nucleon-nucleon potentials, *Phys. Rev. C* **8** (1973) 1164–1166.
[22] A. deShalit and H. Feshbach, *Theoretical Nuclear Physics*, Volume 1, Nuclear Structure, Wiley, New York, 1974.
[23] I.S. Gradshteyn and I.M. Ryzhik, *Table of Integrals, Series, and Products*, Academic Press, London, 1980.
[24] T Hamada and I.D. Johnston, A potential model representation of two-nucleon data below 315 MeV, *Nucl. Phys.* **34** (1962) 382–403.
[25] R.V. Reid, Local phenomenological nucleon-nucleon potentials, *Ann. Phys.* **50** (1968) 411–448.
[26] R.B. Wiringa, V.G. J. Stoks and R. Schiavilla, Accurate nucleon-nucleon potential with charge-independence breaking, *Phys. Rev. C* **51** (1995) 38–51.
[27] S. Weinberg, Nuclear forces from chiral lagrangians, *Phys. Lett. B* **251** (1990) 288–292.
[28] R. Machleidt and D.R. Entem, Chiral effective field theory and nuclear forces, *Phys. Reports* **503** (2011) 1–75.
[29] W. Sturhahn, Nuclear resonant spectroscopy, *J. Phys.: Condensed Matter* **15** (2004) S497–S530.
[30] R. Rüffer and A.I. Chumakov, Nuclear resonance, *Synchrotron Light Sources and Free Electron Lasers Accelerator Physics, Instrumentation and Science Applications*, Springer, Berlin, 2014, pp. 1–32.
[31] A. Q. R. Baron, Introduction to High-Resolution Inelastic X-Ray Scattering, *arXiv preprint* arXiv:1504.01098 (2015).
[32] A.I. Chumakov, A.Q.R. Baron, J. Arthur, S.L. Ruby, G.S. Brown, G.V. Smirnov, U. van Bürck and G. Wortmann, Nuclear scattering of synchrotron radiation by ^{181}Ta, *Phys. Rev. Lett.* **75** (1995) 549–552.
[33] O. Leupold, A.I. Chumakov, E.E. Alp, W. Sturhahn and A.Q.R. Baron, Noniron isotopes, *Hyperfine Interactions* **123/124** (1999) 611–631.
[34] I. Serdons, R. Callens, R. Coussement, S. Gheysen, J. Ladriere, S. Morimoto, S. Nasu, J. Odeurs, Y. Yoda and G. Wortmann, Stroboscopic detection of the ^{181}Ta–Mössbauer resonance with synchrotron radiation, *Nucl. Instr. Methods Phys. Res. B* **251** (2006) 297–303.
[35] G.P. Chambers, J.E. Eridon, K.S. Grabowski, B.D. Sartwell and D.B. Chrisey, Charged particle spectra of palladium thin films during low energy deuterium ion implantation, *J. Fusion Energy 9* (1990) 281–285.
[36] J.R. Huizenga and L.R. Moretto, Nuclear level densities, *Annual Rev. Nucl. Sci.* **22** (1972) 427–464.

[37] A.G. Lipson, G.H. Miley, A.S. Roussetski and E.I. Saunin, Phenomenon of an energetic charged particle emission from hydrogen/deuterium loaded metals, *Proc. ICCF10* (2003) 539–558.
[38] A.G. Lipson, G.H. Miley, B.F. Lyakhov and A.S. Roussetski, Energetic charged particle emission from hydrogen loaded Pd and Ti cathodes and its enhancement by He-4 implantation, *Proc. ICCF11* (2004) 324–338.
[39] A.S. Roussetski, CR-39 track detectors in cold fusion experiments: Review and perspectives, *Proc. ICCF11* (2004) 274–280.
[40] A.G. Lipson, G.H. Miley, A.S. Roussetski, B.F. Lyakhov and E.I. Saunin, Reproducible nuclear emissions from Pd/PdO:Dx heterostructure during controlled exothermic deuterium desorption, *Proc. ICCF12* (2005) 293–313.
[41] A.G. Lipson, A. Roussetski and G.H. Miley, Evidence for condensed matter enhanced nuclear reactions in metals with a high hydrogen solubility, *Proc. ICCF13* (2007) 248–268.
[42] P.A. Mosier-Boss, L.P. Forsley, A.S. Roussetski, A.G. Lipson, F. Tanzella, E.I. Saunin, M. McKubre, B. Earle and D. Zhou, Use of CR-39 detectors to determine the branching ratio in Pd/D co-deposition, *Current Science* **108** (2015) 585–588.
[43] P.A. Mosier-Boss, L.P.G. Forsley and P.K. McDaniel, Investigation of nano-nuclear reactions in condensed matter, *Technical Report for DTRA* (2016).
[44] A.S. Roussetski, Application of CR-39 plastic track detector for detection of DD and DT-reaction products in cold fusion experiments, *Proc. ICCF8* (2000) 253–257.
[45] E. Storms and B. Scanlan, Detection of radiation emitted from LENR, *Proc. ICCF14* (2008) 263–287.
[46] S.A. Lipinski and H.U. Lipinski, Hydrogen–lithium fusion device, methods and applications, *United States Patent Application Publication* US 2009/0274256 A1 (2009).
[47] S.A. Lipinski and H.U. Lipinski, Hydrogen–lithium fusion device, *WIPO/PCT Patent Application Publication* WO 2014/189799 A9 (2014).
[48] X.Z. Li, Z.M. Dong, C.L. Liang, Y.P. Fu, B. Liu, G.S. Huang, S.X. Zheng and S. Chen, Hydrogen-lithium low energy resonant electron-capture and BetheŠs solar energy model, *J. Condensed Matter Nucl. Sci.* **25** (2017) 181–192.
[49] V.P. Chechev and N.K. Kuzmenko, CEA Table de radiounucléides ^{57}Co, Laboratoire National Henri Becquerel LNE-LNHB/CEA Report (2014).
[50] A.I. Chumakov, A.Q. R. Baron, I. Sergueev, C. Strohm, O. Leupold, Y. Shvyd'ko, G.V. Smirnov, R. Rüffer, Y. Inubushi, M. Yabashi, K. Tono, T. Kudo and T. Ishikawa, Superradiance of an ensemble of nuclei excited by a free electron laser, it Nature Physics **14** (2018) 261–265.
[51] F.F. Karpeshin, Resonance internal conversion as a way of accelerating nuclear processes, *Phys. Particles and Nuclei* **37** (2006) 284–305.
[52] V.A. Krutov, Internal conversion in the field of an electronic bridge, *JETP Letters* **52** (1990) 584–588.